Synthesis and radioactive labeling of biologically active peptides, peptide and protein fragments

Ph.D. Thesis

Erzsébet Szemenyei

Institute of Biochemistry
Biological Research Centre of the
Hungarian Academy of Sciences

Szeged
2008

LIST OF PUBLICATIONS RELATED TO THE THESIS

I. **Erzsébet Szemenyei**, Géza Tóth; Tritium labelling and degradation studies of Dmt[1]-endomorphin-2. *Journal of Labelled Compounds and Radiopharmaceuticals*, **50**: 1148-1152, (2007).

II. Veronica Gonzalez-Nuñez, Gemma Arsequell, **Erzsébet Szemenyei**, Géza Tóth, Gregorio Valencia, Raquel E. Rodriguez; Binding profile of the endogenous novel heptapeptide Met-Enkephalin-Gly-Tyr in zebrafish and rat brain. *The Journal of Pharmacology and Experimental Therapeutics*, **314**: 862-867, (2005).

III. András. Z. Rónai, **Erzsébet Szemenyei**, Erzsébet Kató, László Kocsis, György Orosz, Mahmoud Al-Khrasani, Géza Tóth; Endomorphin synthesis in rat brain from intracerebroventricularly injected [^{3}H]-Tyr-Pro: A possible biosynthetic route for endomorphins. *Regulatory Peptides*, **134** (1): 54-60, (2006).

IV. **Erzsébet Szemenyei**, István Barna, Zsuzsa Mergl, Attila Keresztes, Zsuzsanna Darula, Erzsébet Kató, Géza Tóth, András Z. Rónai; Detection of a novel immunoreactive endomorphin 2-like peptide in rat brain extracts. *Regulatory Peptides*, **148**: 54-61, (2008).

V. Archana Mukherjee, Kanchan Kothari, Géza Tóth, **Erzsébet Szemenyei**, Hal Dhar Sarma, József Környei, Meera Venkatesh; ^{99m}Tc-labeled annexin V fragments: a potential SPECT radiopharmaceutical for imaging cell death. *Nuclear Medicine and Biology*, **33** (5): 635-643, (2006).

ACKNOWLEDGEMENTS

I would like to thank my supervisor, Dr. Géza Tóth, for the opportunity to accomplish my PhD work in his laboratory and for all his support during this period.

It is to thank to my university consultant, Dr. Éva Hajdú, and Prof. Botond Penke for all their help.

Dr. András Z. Rónai and Dr. József Környei are entitled extra acknowledgement for their useful professional advices, kind instructions and stable support.

My thanks are due to the members of the pharmacology group of the Semmelweis University, to Dr. Erzsébet Kató and Dr. Mahmoud Al-Khrasani, to Dr. Raquelle Rodriguez's team from University of Salamanca for the biological characterization of my compounds. Special thanks to Dr. Zsuzsa Mergl for the immunization and Dr. István Barna for the radioimmunoassay.

I am grateful to Dr. Kanchan Kothari and her group from Bhabha Atomic Research Centre for the biological measurements of the annexin V fragments.

I am grateful to Dr. Zsuzsanna Darula, Emília Szájli and Dr. Zoltán Kele for the mass-spectrometric analysis of my peptides.

At last but not least, thanks also to be expressed to my colleagues in our laboratory, to Dr. Judit Farkas, Éva Papp, Bencze Jánosné, Andrea Mosonyi, Attila Keresztes, Dr. Attila Borics, Dr. Csaba Tömböly and special thanks to Dr. Balázs Leitgeb.

TABLE OF CONTENTS

LIST OF ABBREVIATIONS

AcOH	acetic acid
ACN	acetonitrile
Anx V	annexin V
Anx13	Ala-Gln-Val-Leu-Arg-Gly-Thr-Val-Thr-Asp-Phe-Pro-Gly
B_{max}	maximal number of binding sites
Boc	*tert*-butyloxylcarbonyl
cDNA	complementary DNA
CT	computed tomography
DCC	N,N'-dicyclohexylcarbodiimide
DCM	dichloromethane
DIC	N,N'-diisopropylcarbodiimide
DIEA	N,N-diisopropylethylamine
DMF	dimethylformamide
DMS	dimethylsufide
Dmt	2',6'-dimethyl-tyrosine
DTT	1,4-dithio-DL-threitol
EDTA	ethylenediaminetetraacetic acid
EM2	endomorphin-2 (Tyr-Pro-Phe-Phe-NH_2)
Dmt^1-EM2	Dmt-endomorphin-2 (Dmt-Pro-Phe-Phe-NH_2)
ESI	electrospray ionization
EtOH	ethanol
Fmoc	9-fluorenylmethoxycarbonyl
HBTU	O-benzotriazol-1-yl-tetramethyl-uronium hexafluorophosphate
HF	hydrogen fluoride
HOBt	N-hydroxybenzotriazole
HYNIC	2-hydrazinonicotinic acid
k'	capacity factor
K_D	dissotiation constant
K_i	equilibrium inhibition constant
LC-MS	liquid chromatography-mass spectrometry
LSC	liquid scintillation counting
MALDI-TOF	matrix-assisted laser desorption/ionization-time of flight

MBHA	4-methylbenzhydrylamine
MEGY	Met-enkephalin-Gly-Tyr (Tyr-Gly-Gly-Phe-Met-Gly-Tyr)
MERF	Met-enkephalin-Arg-Phe (Tyr-Gly-Gly-Phe-Met-Arg-Phe)
icv	intracerebroventricular
ORL_1	opioid receptor-like
PCN	tris(2-cynoethyl)phosphine
PET	positron emission tomography
PNP	bis(dimethoxypropyl-phosphinoethyl) methoxyethylamine
PS	phosphatidylserine
R_f	retention factor
RIA	radioimmunoassay
RP-HPLC	reverse phase high-performance liquid chromatography
SDH	succinic acid dihydrazide
SPECT	single photon emission computed tomography
TEA	triethylamine
TFA	trifluoroacetic acid
TIS	triisopropylsilane
TLC	thin-layer chromatography
Tris.HCl	tris(hydroxymethyl)aminomethane chloride
Tyr-W-MIF-1	Tyr-Pro-Trp-Gly-NH_2
UV	ultraviolet
YP	Tyr-Pro-OH
YPF	Tyr-Pro-Phe-OH
YPW	Tyr-Pro-Trp-OH
YPFF-NH_2	Tyr-Pro-Phe-Phe-NH_2
YPWP-NH_2	Tyr-Pro-Trp-Phe-NH_2
YPFF-OH	Tyr-Pro-Phe-Phe-OH
YPWF-OH	Tyr-Pro-Trp-Phe-OH

1. Introduction

1.1. Radioactive isotopes as tracers

Radioactive tracing

The first experiments with radioactive tracers were conducted in 1913 by György Hevesy and Friedrich A. Paneth who determined the solubility of lead salts by using radium-D, one of the naturally occuring radioactive isotopes of lead. For the development of the *trace method* Hevesy was awarded the Nobel Prize in Chemistry in 1943. The tracer technique came into common use after Word War II when relatively large amounts of cheap artificial radionuclides became available through the use of nuclear reactors.

The largest field of application of radiotracers is in the life sciences. Using of the labeled compounds is significant in the biochemical analysis such as in the autoradiography, the immunoassay, the DNA-analysis and in the direct tracing. The one of the most important user of radionuclides is medical sciences. Currently, the medical imaging techniques, which use radionuclides (Transmission Tomography - CT, Emission Computed Tomography – SPECT, PET) are widely applied diagnostic methods in the medicine. Radiotracers are also used for therapy such as internal or external sources.

What are the advantages and the disadvantages of using radiotracers? The radioactive isotopes are chemically identical with stable isotopes of the same element. The difference in the mass of the nucleus between the various isotopes does cause some change in the chemical and physical properties, but in most cases the isotope effect is rather small and difficult to detect.

Apparently, the radiotracers are easy to detect and measure with high precision to sensitivities of 10^{-16} to 10^{-6} g and the radioactivity is independent of temperature, pressure, chemical and physical state. The radiotracers do not affect the system and can be used in nondestructive techniques and if the tracer is radiochemically pure, interference from other elements is of no concern. For most radioisotopes the radiation can be measured independently of the matrix, eliminating the need for calibration curves (**1**).

Tritium and tritium labeling methods of peptides

Tritium was first predicted in the late 1920s by W. Russell, using his "spiral" periodic table, then produced in 1934 from deuterium, another isotope of hydrogen, by E. Rutherford, working with M. Oliphant and P. Harteck. Rutherford was unable to isolate the tritium, a job that was left to L. Alvarez and R. Cornog (1939) (**2**) who correctly deduced that the substance was radioactive. Upon the bombardment of deuterium with nuclei of deuterium (deuterons) in a cyclotron the following nuclear reactions occurred:

$$^{2}_{1}H + {}^{2}_{1}H \rightarrow {}^{3}_{2}He + {}^{1}_{0}n + 4.04\ MeV$$
$$^{2}_{1}H + {}^{2}_{1}H \rightarrow {}^{3}_{1}H + {}^{1}_{1}H + 3.26\ MeV$$

For convenience, these two reactions may be written as:

$$^{2}H\ (d,n)\ ^{3}He \text{ and } ^{2}H\ (d,p)\ ^{3}H$$

where *d* is a deuteron; *n*, neutron; *p*, proton.

Tritium occurs naturally due to cosmic rays interacting with atmospheric gases. In the most important reaction for natural tritium production, a fast neutron (>4MeV) interacts with atmospheric nitrogen (**3**):

$$^{14}_{7}N + {}^{1}_{0}n \longrightarrow {}^{12}_{6}C + {}^{3}_{1}H$$

Tritium is now produced on a large scale in reactors, where any nuclide can easily be exposed to a high flux of neutrons under controlled conditions. Among the various possibilities it was found that lithium is a particularly favorable nuclide because of its high "cross section" for thermal neutrons. This means that the lithium nucleus splits easily when exposed to neutrons of energy lower than molecular bond energies yielding tritium and a helium nucleus. This reaction is most widely used now to produce tritium in large quantities (**4**-**6**).

$$^{6}\text{Li}\ (n,\alpha)\ ^{3}H$$

Tritium is a fission product within the nuclear fuel, generated at rate of 0.37-0.74 PBq (1-2 $\times$ 10^4 Ci)/year and also produced in heavy water-moderated reactors when deuterium captures a neutron, but this reaction has a small cross section.

Tritium nucleus decays by the emission of an electron (β^--particle) and antineutrino, in which process one of the neutrons changes into a proton. The product of the decay of tritium is a helium ion, the nucleus of which has a mass of 3 and stable. The decay of tritium is therefore a simple one-step process:

$$^{3}H \rightarrow {}^{3}He^{+} + \beta^{-} + \nu_{a}$$

According to W. M. Jones (**7**), the half-life is 12.262 ± 0.004 years. Beta-radiation from a nuclide always occurs in a characteristic spectrum. The spectrum of the radiation of tritium is continuous from zero to a maximum energy. The maximum energy is 18.6 keV and the average energy is close to 5.6 keV. The low-energy β^--particels of tritium can be shielded by the skin, paper, or simply about 6 mm of air.

One milliatom (mmol) of tritium represents a radioactivity of 1.08 TBq (29.18 Ci). Tritium, the most versatile radionuclide in chemical and biochemical research, readily labels

complex organic and bioorganic molecules more so than any other radioisotope (**8)**. Several investigations, *in vitro* receptor studies, biochemical receptor analyses, autoradiographic localization and distribution studies of the receptors and other biodegradation assays are usually based on peptide labeled with tritium.

There are two basic methods for introducing tritium into organic molecules, exchange methods and synthetic methods (**9**). The $^{3}H/H$ isotope exchange reactions do not require separate synthetic steps. The disadvantage of this method is that the compounds are randomly labeled and the high percent of impurities are formed during radiolytic side reactions. Synthetic methods, where tritium is directly and specifically inserted, yield high tritium incorporation, but are limited by the chemistry required. The main methods for the tritium labeling of neuropeptides (**10)** include above-mentioned isotope exchange reactions (β^--radiation induced (**11)**, catalytic (**12**)) and methylation of peptides with ^{3}H-methyl iodide (**13)** or reductive methylation using tritiated metal hydrides (**14**), chemical or enzymatic synthesis from precursor peptides or labeled amino acids. The synthesis of peptides from labeled amino acids is advantegeous, the tritiated amino acids are characterized, the specific activity and position of tritium atoms incorporated into amino acids are known. In case of synthesis of tritiated peptides using precursor peptides, the most important chemical modification is the iodination of peptides. Tyrosine and histidine residues can be iodinated using different methods, for example using I_2 solution in methanol, ICl, *in situ* generated iodine by the reaction of HI and HIO_3 under strong acidic conditions, reaction of chloramine-T with iodide, enzymatic iodination with peroxidase, and reaction of Iodo-Gen® and Iodo-Beads® (**15**). In most cases, the mono-, diiodinated and noniodinated peptides containing reaction mixture should be purified by HPLC. For tritiation, the diiodo analogs are the favorable derivative.

Precursor peptides for tritiation can be obtained by peptide synthesis using amino acid derivatives containing halogens, double or triple bonds. The most frequently used amino acids are 3',5'-diiodotyrosine and 3',5'-dibromotyrosine, although tritium labeling at *ortho* position to OH group are more labile than at *meta* positions. Using *p*-iodophenylalanine or other *para*-halogenated phenylalanine for precursor synthesis, the specific activity will be less in the tritiated peptide, but the label is more stable (**16)**. Tritium can be incorporated into histidine or tryptophan using 2',4'-diiodohistidine-(**17***)* or 5',7'-dibromotryptophan-containing peptides (**18***)*, respectively. Peptides containing dehydroproline, dehydroleucine, dehydroisoleucine, propargyl, or allyl-glycine are also frequently used as precursors. (**Figure 1.**)

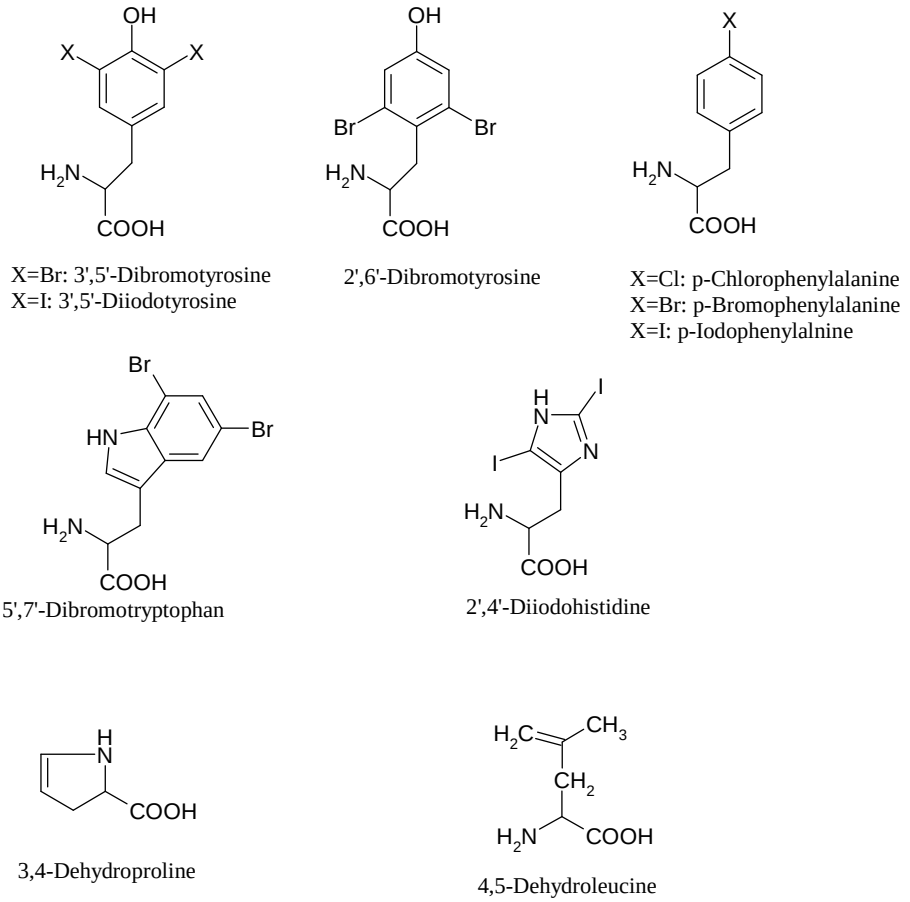

Figure 1. Amino acid derivatives used for synthesis of precursor peptides for tritiation

Technetium-99m and ^{99m}Tc- labeling methods of peptides

C. Perrier and E. Segré in 1937 discovered the element of atomic number 43, isolated by deuteron bombardment of molybdenum (**19,20**). The nuclear and chemical properties of this missing element, *eka-manganese*, were predicted by D. Mendeleev. This element was also isolable in larger amounts from the fission products of uranium (**21**). The name *technetium* was coined by F. A. Paneth (**22**) from the Greek *τεχνητός* to denote that this was the first artificial element made by man, and the chemical symbol was suggested to be Tc. Nuclear isomerism of the element Tc and the existence of ^{99m}Tc were discovered by G. T. Seaborg and E. Segré (**23**).

^{99m}Tc in some chemical form is used in more than 85% of the diagnostic scans done each year in hospitals. The nuclear properties of ^{99m}Tc are virtually ideal for diagnostic imaging. ^{99m}Tc emits a 140 keV γ-ray with 89% abundance which is close to optimum for imaging with gamma cameras found in most hospitals. Its 6 h half-life is sufficiently long to synthesize the ^{99m}Tc-labeled radiopharmaceuticals, assay them for purity, inject them into the patient, and perform the imaging studies yet short enough to minimize the radiation dose to

the patient. The metastable (a state where the nucleus is in an excited state) isotope, ^{99m}Tc is produced as a fission product from the fission of uranium or plutonium in nuclear reactors, but the vast majority of the ^{99m}Tc is formed from ^{99}Mo which is formed by the neutron activation of ^{98}Mo. ^{99}Mo has a half-life of 66 hours, so short-lived ^{99m}Tc, which results from its decay, is being constantly produced (**24)**. ^{99m}Tc decays to ^{99}Tc.

$$^{98}_{42}\mathrm{Mo} + {}^{1}_{0}\mathrm{n} \longrightarrow {}^{99}_{42}\mathrm{Mo} + \text{gamma-ray}$$

$$^{99}_{42}\mathrm{Mo} \longrightarrow {}^{99m}_{43}\mathrm{Tc} + \text{beta-particle}$$

$$^{99m}_{43}\mathrm{Tc} \longrightarrow {}^{99}_{43}\mathrm{Tc} + \text{gamma-ray}$$

$$MoO_3 + H_2O \rightarrow H_2MoO_4 \ (\ ^{99}MoO_4^-/\ ^{99m}TcO_4^-)$$

The inconvenience of purchasing a short half-life radionuclide was overcome by the development of the ^{99}Mo-^{99m}Tc generator ("technetium cow," also occasionally called a molybdenum cow) (**25**), which takes advantage of the transient equilibrium between the parent radionuclide ^{99}Mo (66 h half-life) and the daughter radionuclide ^{99m}Tc (6 h half-life). The separation of ^{99m}Tc from ^{99}Mo is accomplished by the selective elution of $^{99m}TcO_4^-$ with sterile saline from alumina column containing $^{99}MoO_4^-$. The transient equilibrium results in optimum isolation of maximum ^{99m}Tc activity with minimal ^{99}Tc buildup every 23-24 h. The development of the ^{99}Mo-^{99m}Tc generator allowed this radionulide to become both routinely available and economical.

Klaus Schwochau's book *Technetium* lists 31 radiopharmaceuticals, based on ^{99m}Tc for imaging, functional studies of the brain, myocardium, thyroid, lungs, liver, gall bladder, kidneys, skeleton, blood and tumors.

^{99m}Tc-labeling is still an attractive approach for radiolabeling peptides for nuclear medicine imaging due to its ideal physical characteristics for SPECT and readily availability from a generator. Technetium exhibits a rich and diverse redox chemistry because of its capability of existing in 8 different oxidation states ranging from -1 to +7 (**26**). The Tc(VII) in $^{99m}TcO_4^-$ has to be reduced to a lower oxidation state in order to produce a stable ^{99m}Tc-peptide complex or to a reactive intermediate complex. When $^{99m}TcO_4^-$ is reduced, the oxidation state of technetium depends on the nature of the reducing agent, the chelator, and reaction conditions.

Peptides contain a number of possible active side chains such as the ω-amino group from lysine, phenol moiety from tyrosine, thiol group from cysteine and carboxylate group

from aspartic or glutamic acid. These reactive groups can serve as “handles” for the attachment of a bifuntional coupling agent (**27**).

Abrams and co-workers first reported the use of ^{99m}Tc-HYNIC (2-hydrazinonicotinic acid) core for the ^{99m}Tc-labeling (**28**). Since then, the ^{99m}Tc-HYNIC core has been used for ^{99m}Tc-labeling of chemotactic peptides (**29**). The HYNIC can only occupy one or two coordination sites the square pyramidal or octahedral coordination sphere of the technetium. The advantage of using HYNIC as the bifuntional coupling agent is its high labeling efficiency and the choice of various coligands. The a N atom of HYNIC is coordinated to Tc, forming a –HN-N=Tc bond. The octahedral geometry of the complex is built 4 chelating groups coming from a tetradentate ligand. Several modifications of the HYNIC core were also accomplished by using a tridentate ligand such as tricine as the coligand and a monodentate ancillary ligand (**30**). ^{99m}Tc complexes containing a terminal Tc≡N multiple bond are currently easily produced at tracer level, after the advent of improved chemical methods for obtaining the $[^{99m}Tc{\equiv}N]^{2+}$ core in high radiochemical purity. A key advantage of using this type of complexes for obtaining novel classes of diagnostic agents comes from their intrinsic structural robustness (**31**). This method is based on the reaction depicted in Equation 1, where D is a donor of the nitride nitrogen atoms (N^{3-}), belonging to the class of derivatives of dithiocarbazic acid ($H_2N{-}NH{-}CS_2H$) or, in general, of derivatives containing the –N–N– functional moiety, and R is a reducing agent such as $SnCl_2$ or a tertiary phosphine and HCl (**32**).

$$[^{99m}TcO_4]^- + D + R \rightarrow [^{99m}Tc{\equiv}N] \qquad (1)$$

Through Reaction 1, pertechnetate is quantitatively converted into a mixture of complexes, all of which contain the Tc≡N group. Subsequent addition of a suitable ligand to this mixture leads to the high-yield formation of a single compound in which the terminal metal-nitrogen multiple bond is retained. The high affinity of the Tc≡N core for sulfur donors makes it particularly suitable for linking to peptides having S^- as donor atoms. Experiments conducted with short peptide sequences having a cysteine residue placed in a terminal position of the amino acid chain, indicate that two peptide ligands can bind efficiently around the Tc≡N group via the cysteine, through the thiolate sulfur atom and the amine nitrogen atom. The resulting complexes have the expected square-pyramidal geometry.

Iodine-125 and ^{125}I- labeling methods of peptides

Iodine is an essential trace element; its only known roles in biology are as constituents of the thyroid hormones, thyroxine (T4) and triiodothyronine (T3). There are 37 isotopes of iodine and only one, ^{127}I, is stable (Some selected isotopes of iodine can be seen in **Table 1.**).

^{125}I is widely used as a tracer in biology and medicine. Some current applications include biodistribution studies of ^{125}I-labeled drugs, peptides and antibodies, and the use of ^{125}I-labeled nucleic acid precursors in cell-targeted therapeutics (**33**,**34**). ^{125}I is the most commonly used radio-isotope in radioimmunoassay. The use of ^{125}I as an alternative label has considerable advantages. ^{125}I has a half-life of 60.14 days and decays by 100% electron capture to the first excited state of ^{125}Te. De-excitation from this level to the ground state of stable ^{125}Te is highly converted and the 35.5 keV γ-ray emission occurs only in 7% of the total disintegrations. 93% of the disintegration takes place by internal conversion, which follow photon (X-ray) and Auger electron emissions. The energy averaged over all photons (X- and γ-rays) in the decay of ^{125}I is 26.4 keV (**35**).

$$^{125}I + e^{-} \rightarrow {}^{125m}Te \rightarrow {}^{125}Te + \nu$$

^{125}I is obtained by the neutron irradiation of ^{124}Xe and it is measured with high efficiency by crystal scintillation counting. As a tracer for investigating chemical and biological systems, ^{125}I has clear advantages. The long half-life enables the system to be kept under observation over long periods. Considerable confidence may be placed in the purity of the labeled compound used, as more time is available for thorough purification and analysis, and radiation damage is generally negligible. Compound labeled with ^{125}I are more stable than those correspondingly labeled with ^{131}I, as would be expected from the lack of β^- emission form ^{125}I.

Isotope	Natural abundance	Half-life	Radioactive decay/radiation	β^--particle and γ-energy (MeV)	Decay product
^{125}I	synthetic	60.14 d	Electron capture	-	^{125} Te
			γ-ray	0.035	-
^{127}I	100%	I is stable with 74 neutrons			
^{129}I	synthetic	15.7 x 10^6 y	β^-	0.15	^{129}Xe
^{131}I	synthetic	8.02 d	γ-ray, β^-	0.36, 0.61	^{131}Xe

Table 1. Selected isotopes of iodine (**36**).

Peptide radioiodination is a technique commonly used for *in vitro* radioligand investigations as well as for medical imaging and therapy. Several direct and indirect iodination procedures currently exist. The most widely used direct labeling techniques are based on radioiodination of tyrosine and histidine amino acid residues with chloramine-T (**37**), Iodo-Gen® (1,3,4,6-tetrachloro-3α,6α-diphenylglycoluril) (**38**), lactoperoxidase (**39**), and the related solid-state variants Iodo-Beads® (**40**) or Enzymobeads® (**41**). An alternative method to direct iodination is the conjugation of the peptide with a small radioiodinated molecule such as the Bolton-Hunter reagent (*N*-hydroxysuccinimide ester of 3-(4-hydroxyphenyl)propionic acid) (**42**). These indirect labeling methods are used in case of

absence of tyrosine and histidine residues or when these amino acids are necessary for the peptide activity.

1.2. Endogenous opioids

Opioid receptors and endogenous opioid peptides

The opium, derived from the poppy plant, *papaver somniferum*, has been used for many hundreds of years to relieve pain. In 1803, Sertürner isolated a crystaline sample of the main constituent alkaloid of the crude opium, morphine, which was named after the Greek god of dreams, Morpheus. The structure of morphine was predicted by Gulland and Robinson and the Robinson`s structure was confimed by chemical synthesis (**43**).

Opioids are the most powerful analgesic drugs available, and are the treatment of choice for the management of moderate to severe pain (**44**). The rigid structural and stereochemical requirements essential for the analgesic effect of morphine and related opioids led to the theory that they produce their effects by interacting with a specific receptor (**45**). Side effects, including respiratory depression, nausea, and constipation, impact their use and protracted opioid therapy leads to drug tolerance and physical dependence.

The opioid receptors displayed heterogenous properties, and at least three types of opioid receptors existed, classified as μ-, δ- and κ-receptors (**46**), and these receptors have been confirmed by molecular cloning (**47**-**50**). All of the cloned opioid receptors possess the same general structure of an extracellular N-terminal region, seven transmembrane domains and intracellular C-terminal tail structure. There is pharmacological evidence for subtypes of each receptor and other types of novel, less well-characterised opioid receptors, ε, λ, ι, ζ. More recently, an „orphan" receptor was identified which has a high degree of homology to the „classical" opioid receptors; on structural grounds this receptor is an opioid receptor and has been named ORL_1 (opioid receptor –like) (**51**).

Brain opioid peptide systems are known to play an important role in motivation, emotion, attachment behaviour, the response to stress and pain, and the control of food intake.

In mammalian the endogenous opioid peptides are mainly derived from four precursors: pro-opiomelanocortin, pro-enkephalin, pro-dynorphin and pro-nociceptin/orphanin FQ (**52**-**55**). (**Table 2.**) β-endorphin is equiactive at μ-and δ-receptors with much lower affinity for κ-receptors (**56**). [Met]-and [Leu] enkephalin have high affinities for δ-receptors, ten-fold lower affinities for μ-receptors, but Metorphamide, which is a [Met]-enkephalin derivative displaying highest affinity for the μ-receptor (**57**). The opioid fragments of pro-dynorphin, perticularly dynorphin A and dynorphin B, have high affinity for κ-receptors but also have significant affinity for μ-and δ-receptors (**57**). Nociceptin/OrphaninFQ is the endogenous

ligand for the ORL_1-receptor; it has little affinity for the μ-, δ- and κ-receptors (**55**,**58**). Endomorphins, endomorphin 1 (Tyr-Pro-Trp-Phe-NH_2) and endomorphin 2 (Tyr-Pro-Phe-Phe-NH_2) are two endogenous opioid tetrapeptides with the highest known affinity and specificity for the μ-opioid receptor (**59**). It is assumed that endomorphins are the cleavage products of a larger precursor, but this polypeptide or protein has not yet been identified.

Precursor Protein	**Opioid peptide**	**Amino acid sequence**	**Receptor selectivity**
Pro-opiomelanocortin	α-Endorphin	YGGFMTSEKSQTPLVT	$\mu > \delta >> \kappa$
	β-Endorphin	YGGFMTSEKSQTPLVTL FKNAIIKNAYKKGE	
	γ-Endorphin	YGGFMTSEKSQTPLVTL	
Pro-enkephalin	[Met]enkephalin	YGGFM	$\mu \sim \delta >> \kappa$
	[Leu]enkephalin	YGGFL	$\delta > \mu >> \kappa$
	[Met]enkephalin-Arg^6-Phe^7	YGGFMRF	κ_2
	[Met]enkephalin-Arg^6-Gly^7-Leu^8	YGGFMRGL	κ
	Metorphamide	YGGFMRRV-NH_2	μ
Prodynorphin	Dynorphin A (1-8)	YGGFLRRI	$\kappa > \delta \sim \mu$
	Dynorphin A (1-13)	YGGFLRRIRPKLK	$\kappa > \delta \sim \mu$
	Dynorphin A	YGGFLRRIRPKLKWDNQ	κ
	Dynorphin B	YGGFLRRQFKVVT	κ
	α-neoendorphin	YGGFLRKYPK	
	β-neoendorphin	YGGFLRKYP	
Pronociceptin/OFQ	Nociceptin	FGGFTGARKSARKLANQ	ORL_1
-	Endomorphin 1	YPWF-NH_2	μ
	Endomorphin 2	YPFF-NH_2	μ
Others	Tyr-MIF-1	YPLG-NH_2	μ
	Tyr-W-MIF-1	YPWG-NH_2	μ
	Deltorphin I	YaFDVVG-NH_2	δ
	Deltorphin II	YaFEVVG-NH_2	δ
	Dermenkephalin	YmFHLMD-NH_2	δ
	Dermorphin	YaFGYPS-NH_2	μ

A: Ala, D: Asp, E: Glu, F: Phe, G: Gly, I: Ile, K: Lys, L: Leu, M: Met, N: Asn, P: Pro, Q: Gln, R: Arg, S: Ser, T: Thr, V: Val, W: Trp, Y: Tyr, a: D-Ala, m: D-Met

Table 2. Endogenous opioid peptides

Proteolysis of some functional proteins in vitro leads to the generation of peptides exhibiting an opioid like activity when they have a Tyr-Pro N-terminus sequence. Thus β-casomorphins are released from β-casein (**60**), and hemorphins from hemoglobin (**61**) by in vitro peptic hydrolysis. β-casomorphins are a specific group of milk peptides with biological activity of μ-δ- and κ-opioid receptor agonists (**62**,**63**). The members of the hemorphin family include peptides from 4 to 10 amino acids, which are generated by proteolytic degradation of

the [32-41] segment of human hemoglobin β-chain or [31-40] segment of the bovine hemoglobin β-chain (**64**,**65,66**). (**Table 3**.)

In 1980, two opioid peptides, dermorphin (Tyr-D-Ala-Phe-Gly-Tyr-Pro-Ser-NH_2) and Hyp^6-dermorphin were isolated from the skin of several amphibians (**67**). These heptapeptides were shown to have high affinity and selectivity for the μ-receptors (**68**,**69**). On a molar basis, the analgesic potency of dermorphin is about 1000 times greater than that of morphine (**70**).

Precursor	Endogenous peptide	Amino acid sequence
β-casein (bovine)	β-Casomorphin 5	YPFPG
	β-Casomorphin 7	YPFPGPI
	Morphiceptin	YPFP-NH_2
β-casein (human)	β-Casomorphin 5	YPFV
	β-Casomorphin 7	YPFVEPI
Hemoglobin	LVV-Hemorphin-7	LVVYPWTQRF
	VV-Hemorphin-7	VVYPWTQRF
	Hemorphin-7	YPWTQRF
	VV-Hemorphin-6	VVYPWTQR
	VV-Hemorphin-5	VVYPWTQ
	Hemorphin-5	YPWTQ
	Hemorphin-4	YPWT

Table 3. Other mammalian opioid peptides

Two distinct isoforms (prepro-xendorphin A and B) of an opioid propeptide were isolated from a *Xenopus laevis* brain cDNA library (**71**). Two potential mature peptides, xendorphin-1A and -1B, showed opioid agonist activity and xendorphin 1B (Tyr-Gly-Gly-Phe-Ile-Arg-Lys-Pro-Asp-Lys-Tyr-Lys-Phe-Leu-Asn-Ala) binds with high affinity and specificity to κ-receptors (**72**).

Endomorphins

In 1997, J. E. Zadina and coworkers synthesized a number of Tyr-W-MIF-1 analogs, containing all possible natural substitutions at position 4, which were subsequently screened for the opioid receptor binding. A biologically potent sequence, Tyr-Pro-Trp-Phe-NH_2 was discovered and then identified in the bovine brain and human cortex (**59**,**73**). This peptide named endomorphin 1. a second peptide, Tyr-Pro-Phe-Phe-NH_2, named endomorphin 2, which differs by one amino acid from endomorphin 1 was also isolated. Endomorphins were the first peptides isolated from brain that bind to the μ-opioid receptor with high affinity and selectivity and therefore were proposed as endogenous μ-opioid receptor ligands (**59**). However, the biosynthetic pathways for other vertebrate opioid peptides have already been clarified, their precursor(s) or the possible biosynthetic route(s) still remain(s) unidentified. Endomorphin 1 is widely and densely distributed throughout the brain and upper brainstem and is particularly abundant in the nucleus accumbens (Nac), the cortex, the amygdala, the

thalamus, the hypothalamus, the striatum, and the dorsal root ganglia (**74**,**75**). In contrast, endomorphin 2 is more prevalent in the spinal cord and lower brainstem, endomorphin 2-immunoreactive cell bodies were most prominent in the hypothalamus and the nucleus of the solitary tract (NTS), whereas endomorphin 2-immunoreactive varicose fibers were mainly observed in the substantia gelatinosa of the medulla and the spinal cord dorsal horn (**74**,**76**).

The studies in vivo showed that there are two groups of enzymes mainly responsible for the degradation of endomorphins: dipeptidyl-aminopeptidase IV (DPP IV), which triggers the process, and aminopeptidases, which are involved in secondary cleavage (**77**,**78**). Endomorphins are degraded by similar pathways.

The first step in their catabolism is the cleavage of Pro^2–Trp^3 and Pro^2–Phe^3 peptide bonds, respectively, and the dipeptides formed are then hydrolyzed into amino acids (**79**,**80**). However, the degradation of endomorphin 1 contains an additional minor route: the Tyr^1–Pro^2 peptide bond might also be cleaved in the first step of the enzymatic degradation pathway. There is another degradation pathway of endomorphins, when carboxypeptidase Y and proteinase A hydrolyze endomorphins into peptide acids, releasing ammonia, and then cleave off the C-terminal Phe (**81**,**82**).

Dmt-endomorphins

Endomorphins exhibited the highest affinity for the μ-opioid receptor and extraordinarily high selectivity relative to the δ- and κ-opioid receptor systems of all known opioid substances (**59**,**83**). Hitherto a great number of endomorphin analogues were synthesized (**84**,**85**) Here only one analogue is paraphrazed from the populous endomorphin derivatives. Studies on opioid peptides demonstrated that the introduction of 2',6'-dimethyl-tyrosine (Dmt) in lieu of the common N-terminal Tyr residue in opioid ligands resulted in an exceptional improvement in receptor affinity and functional bioactivity in a wide variety of opioid peptides (**86**-**94**). The substitution of Dmt for Tyr in endomorphin 2 (Dmt^1-endomorphin 2) resulted in one of the most active peptides among several analogues containing an alkyl-modified aromatic ring of Tyr (**95**,**96**). Dmt increased μ-opioid receptor affinity and μ-opioid receptor bioactivity of endomorphin 2 by 5- and 83-fold, respectively The δ-affinity and bioactivity of Dmt^1-endomorphin 2 increased 2 to 3 orders of magnitude, thereby transforming once highly selective ligand into a bivalent or bifuntional opioid peptide derivative (**95**,**96**).

By means of the building of Dmt into the first position, the increased hydrophobicity and alteration in conformation might enhance receptor interaction through π–π stacking, stabilization of hydrophobic interactions with aliphatic or aromatic side-chains in the receptor, and strengthen hydrogen bonding capabilities of the hydroxyl group (**97**,**98**).

Zebrafish endogenous opioid peptide

Zebrafish, *Danio rerio* is considered a model organism (**99**), not only for the study of the biological functions of vertebrates but also as a tool to analyze the effects of some drugs or toxic agents (**100-102**). Five zebrafish opioid precursor genes homologous to the mammalian opioid propeptide genes have recently been identified (**103-105**). These precursors contain novel opioid peptides that can display different pharmacological properties than their counterparts in mammals. In particular, mammals present an enlarged form of Met-enkephalin [Met-enkephalin-Arg-Phe (MERF)] that is different from its homolog in zebrafish, the Met-enkephalin-Gly-Tyr (MEGY).

1.3. Role of Annexin V in apoptosis

Apoptosis

Apoptosis is a form of programmed cell death in multicellular organisms. It is one of the main types of programmed cell death (PCD) (**106**), and involves a series of biochemical events leading to a characteristic cell morphology and death: more specifically, a series of biochemical events which lead to a variety of morphological changes, including blebbing, changes to the cell membrane such as loss of membrane asymmetry and attachment, cell shrinkage, nuclear fragmentation, chromatin condensation and chromosomal DNA fragmentation (1-4). Processes of disposal of cellular debris whose results do not damage the organism differentiates apoptosis from necrosis. Apoptosis (Greek: *apo* - from, *ptosis* - falling) was distinguished from traumatic cell death by J. F. Kerr while he was studying tissues using electron microscopy (**107**,**108**).

Apoptosis can occur when a cell is damaged beyond repair, infected with a virus, or undergoing stress conditions such as starvation. DNA damage from ionizing radiation or toxic chemicals can also induce apoptosis via the actions of the tumour-suppressing gene *p53*. Apoptosis also plays a role in preventing cancer; if a cell is unable to undergo apoptosis, due to mutation or biochemical inhibition, it can continue dividing and develop into a tumour.

Dying cells that undergo the final stages of apoptosis display phagocytotic molecules, such as phosphatidylserine (PS), on their cell surface (**109**,**110**). PS is normally found on the cytosolic surface of the plasma membrane, but is redistributed during apoptosis to the extracellular surface by a hypothetical protein known as scramblase (**111**). These molecules mark the cell for phagocytosis by cells possessing the appropriate receptors, such as macrophages (**112**).

Annexin V

Many drugs, such as cytostatic agents, induce a therapeutic effect through the activation of programmed cell death in target cells (**106**). The detection and quantification of apoptosis

in vivo are of significant clinical value for diagnosis and assessment of therapeutic efficacy. In the last decade, a molecular imaging protocol was developed to measure the programmed cell death *in vitro* and *in vivo* in animal modells and patients (**113**-**116**). This imaging protocol is based on the facts that apoptotic cells externalize the negatively charged phospholipid (PS) and that the human protein Annexin V binds to PS selectively and with a high affinity (**117**).

Anx V, a protein with a molecular weight of 36 kDa is a member of annexin family. This is a multiprotein family of over 160 proteins that share the property of Ca^{2+}-dependent binding to negatively charged phospholipid surfaces (**118**). Annexins are located mainly intracellularly, but AnxV can also be secreted and detected on the outer surface of plasma membranes (**119**). AnxV consists of 319 amino acids and the molecule is arranged in planar cyclic structure of 4 domains (**120**,**121**). The binding of AnxV to phospholipids is very rapid, extremly dependent on the presence of Ca^{2+} and reversible in the presence of the ion chelator EDTA. Studies with PS-containing liposomes found that the stoichiometry of AnxV binding to PS ranges between 4 and 8 AnxV molecules per one PS molecule (**122**,**123**). The Anx V affinity assay was further developed by labeling Anx V with biotin or with radionuclides to enable various protocols for measuring apoptosis *in vitro* (**124**) and *in vivo* (**125**-**127**) animal models.

Radionuclide imaging with radiolabeled annexin V is a highly specific technique that enables delineation of apoptotic areas with good resolution (**128**). AnxV has been tagged with several radionuclides such as ^{99m}Tc (**129**–**131**), ^{18}F (**132**,**133**), ^{64}Cu (**134**) and $^{123/124}$I (**135**–**138**) to detect cell death in vivo by SPECT or PET imaging. ^{99m}Tc-HYNIC-Anx V has been used to detect apoptosis in vivo with gamma camera imaging and SPECT (**139**,**140**).

2. Aims and Scopes

Radioactive tracers have applications in medicine, research, indusrty, agriculture, and many other fields of science and technology.

Tritium labeled biologically active peptides are valuable tools for biological characterization of receptors, and binding sites. The metabolic pathway of tritium labeled compounds is also easily traceable. Our aim was to acquire suitable tools for use in *in vitro* and *in vivo* biological assays.

Two Dmt^1-EM2 isotopomers were labeled with tritium in position 1 or position 2. The isotopomers may become a useful ligands for direct radioreceptor binding and may serve as important tools for degradation studies in rat brain homogenates.

We aimed to prepare an eligible tool for characterizing of the binding profile of MEGY peptide in zebrafish, the organism in which this peptide is naturally present as an endogenous opioid ligand. To achieve this objective, we have synthesized and labeled the MEGY peptide and our biologist cooperators (Dr. Raquelle Rodriguez's team from University of Salamanca) performed binding assays. Two MEGY analogs were also synthesized: (D-Ala^2)-MEGY (Y-D-Ala-GFMGY) and (D-Ala^2, Val^5)-MEGY (Y-D-Ala-GFVGY). The change of a Gly by a D-Ala may confer resistance against proteases such as dipeptidyl-aminopeptidases, which remove the N-terminal dipeptide Tyr^1-Gly^2. In addition, the substitution of Met by Val may help to determine the importance of the methionine residue for the specific opioid binding.

The biosynthetic pathways for other vertebrate opioid peptides have already been clarified (it happens through a single- or multi-step cleavage from large molecular weight precursors with or without additional post-translational modifications), the biosynthetic route of endomorphins is still obscure. Based on the hypothesis that biosynthesis of an oligopeptide may take place also from its fragments through a specific enzymatic route, we decided to label Tyr-Pro dipeptide with tritium and test using HPLC combined with radiodetection the probable incorporation of *icv* injected [^{3}H]Tyr-Pro into endomorphin-related peptides in the rat brain. In addition we aimed to develop a RIA to endomorphin 2, therefore we raised antibodies to EM2-keyhole limpet hemocyanine conjugate in rabbits and labeled EM2 with ^{125}I isotope.

Imaging apoptosis has many applications with new ones emerging with time. The most widely used application is in cancer treatment for assessing tumor response to novel therapies as tumor often respond to radiation as well as to chemotherapy by direct induction of apoptosis. ^{99m}Tc labeled annexin V is considered as an useful tool for apoptosis detection but it has many disadvantages from point of view of radiopharmaceutical kit formulation and agents with faster urinary excretion are also required for routine clinical applications. We

tried to focus on the development of phosphatidyl-serine specific small ^{99m}Tc-labeled annexin V fragments for apoptosis imaging. Annexin type proteins generally possess their biospecific sequences on the N-terminal and in case of Annexin V, the phosphatidyl-serine specific sequency might be attributed to a chain on the N-terminal consisting of 13 amino acids. Based on this concept, a peptide containing particular sequence of these 13 amino acids (Anx13) was designed and derivatized with cisteine and two cisteine for novel ^{99m}Tc-nitrido labeling method and additional two Anx13 derivatives was designed by attachment of histidine and hydrazino nicotinic acid residues for tricarbonyl, HYNIC labeling approaches (respectively).

3. Materials and Methods

Protected and unprotected amino acids and resins were purchased from Sigma-Aldrich, Calbiochem-Novabiochem or Bachem. Coupling agents were from Fluka and Senn Chemicals. Trifluoroacetic acid (TFA), catalyst, TLC plates (Silica gel 60 F_{254}), and solvents were fom Merck and Sigma-Aldrich. $Na^{125}I$ and $^{99m}TcO_4$ were purchased from Institute of Isotopes Co. Ltd. $^3H_2$ was purchased from Technobexport, Russia. Fluorenylmethyloxycarbonyl-hydrazinonicotinic acid (Fmoc-HYNIC) was synthesized in our laboratory.

HF cleavage was performed using a standard apparatus from Peninsula Laboratories, Inc. The following solvent systems were used for TLC analysis: acetonitrile:methanol:water (4:1:1); 1-butanol-acetic acid-water (4:1:1); ethyl acetate:pyridine:acetic acid:water (60:20:6:11,). Ninhydrin, UV light and iodine vapor were employed to detect the peptides and amino acids on the thin layer.

RP-HPLC was performed on Merck-Hitachi or Merck-Lachrom RP-HPLC system, utilizing Vydac 218TP1010 C18 (250 × 10 mm, 10 μm) semipreparative column for preparative purposes, and Vydac 218TP54 C18 (250 × 4.6 mm, 5 μm) column for analytical purposes. Peptides were detected by UV at 215 or 280 nm. The following solvents were used: solvent A was 0.08 % TFA/acetonitrile and solvent B was 0.1% TFA/water.

Molar mass of the peptides were determined and LC-MS or MS analyses were carried out by ESI mass spectrometry (Finnigan TSQ 7000 or Shimadzu QP 80000) and MALDI-TOF mass spectrometry (Bruker Reflex III).

Working with tritium

In biological material, 50 % of the tritium β-particles are calculated to be absorbed already by a layer only 0.3 μm thick, 80 % of the particles are calculated to be absorbed within 1 μm from the source, and 99 % of the radiation does not reach beyond 2.5 μm. Therefore the work with tritium does not require the using of the shielding. Tritium can be absorbed easily through the skin or by inhalation. Lab coat and gloves provide efficient protection in preventing skin contact with contaminated surfaces. After any potential skin exposure the skin should be decontaminated as soon as possible in order to minimize absorption into the body. Effective personal decontamination methods include rinsing the affected part of the body with cold water and soap. Cold water keeps the pores of the skin closed and reduced the transfer of ^3HHO across the skin.

Tritiation reactions were carried out on our self-designed vacuum manifold described earlier (**10**). Our lab has a Triton β-gas monitor (Johnston laboratories Inc.) for low level detection and measurement of tritium gas in the air.

Tritium-labeled materials were analysed and purifield on an RP-HPLC (Jasco) instrument using Vydac 218TP54 C18 (0.46 × 25 cm, 5 μm) or Merck 50943 LiChroCART (124-4 LiChrospher 100 RP-18 , 5 μm) column, detected by a Jasco UV-975 spectrometer and a Canberra Packard 505 TR Flow Radiochromatography Detector. Radioactivity was counted in toluene-Triton X-100 or Ultima Gold scintillation cocktail with a Packard TRI-CARB 2100 TR Liquid Scintillation Analyzer.

Working with ^{125}I and ^{99m}Tc

Iodine-125 is an electron capture radionuclide emitting low energy X and gamma radiation with 35.5 keV energy. Due to the volatile nature of iodine, the most significant hazard is from inhalation, the critical organ for uptake is the thyroid. Iodine-labeled compounds can penetrate surgical rubber gloves. Two pair should be worn, or polythene over rubber. Direct handling of ^{125}I is to be avoided, forceps, shielded syringes must be used. Low activity RIA kits (< 370 kBq) may normally be handled on the open bench, but all other work with iodine should be carried out in a fume cupboard. For work with higher activities special transparent shielding made from lead impregnated acrylic to be necessary which has a lead equivalence value of 0.5 mm. Sample pots containing ^{125}I should be shielded with 1 mm of lead. Solutions containing iodide ions should neither be made acidic nor stored frozen, both lead to formation of volatile elemental iodine. An alkaline solution of 5% sodium thiosulphate should be used to render the spill chemically stable, prior to decontamination by the normal methods. In the case of an accident involving possible ingestion/inhalation of radioiodine may be possible to block uptake to the thyroid by the administration of potassium iodide tablets. (200 mg given two hours after ingestion will reduce uptake by 80%).

The gamma ray average energy of ^{99m}Tc is 140.5 keV and it also emits X-ray with 18 keV and 21 keV energy. Technetium-99m is a decay product of molybdenum-99 and is obtained in solution form by eluting it from a molybdenum-99 “cow”. The recommended protective clothing are lab coat (which must be monitored before leaving the laboratory), disposable plastic, latex or rubber gloves, footwear covers. Waterproof gloves should be worn during elution. The dispensing of the ^{99m}Tc should be carried out in a lead shielded box and during the work wearing of lead apron is recommeded. Personal decontamination techniques are following: washing of the contaminated part of the body with soap and water and after monitoring of the skin. Decontamination of clothing and surfaces are covered under operating and emergency procedures.

3.1. Synthesis and purification of peptides

Peptides were synthesized manually by solid phase-peptide synthesis using either Boc or Fmoc chemistry.

Solid-phase peptide synthesis using Boc strategy

Peptide synthesis using Boc protocol was carried out on 4-methylbenzhydrylamine (MBHA) resin for peptide amides or on Merrifield resin for peptide acids. Attachment of the first Boc-protected amino acid to the chloromethyl resin was performed by using Gisin method (**142**). The synthesis protocol is summarized in **Table 4**.

Step	Reagent	Time
Washing	DCM	3 × 1 min
Deprotection	50% TFA, 2% anisole/DCM	1 × 2 min and 1 × 20 min
Washing	DCM	3 × 1 min
Neutralization	10% DIEA/DCM	2 × 2 min
Washing	DCM	3 × 1 min
Kaiser test		
Coupling	2 eq. Boc-amino acid, 2 eq. DCC, 2 eq. HOBt	60 min
Kaiser test		
Washing	DCM, EtOH	3 × 1 min, 3 ×1 min

Table 4. General schedule for peptide synthesis using Boc chemistry

For methionine or tryptophane containing peptides the deprotection mixture contained 0.5% DTT. Coupling reactions were carried out after the neutralization step with 2 equivalents of Boc-AA, HOBt and DCC in DCM until negative Kaiser test (**143**). Hydroxybenzotriazole esters of protected amino acids are easily formed from DCC or DIC/HOBt *in situ*. After the last washing step the peptide-resin was dried under vacuum. Final deprotection and cleavage from the resin were carried out by HF.

In general, HF cleavage reactions were performed between -5°C – 0 °C, for 60 minutes. The following cleavage mixtures have been used: for peptides containing cysteine: HF/DMS/anisole/p-thiocresol (10:1:1:0.2) and for other peptides HF/DMS/anisole (10:1:1). After completion of the cleavage reaction, HF was evaporated from the peptid-resin mixture. To prevent side ractions during this process, it was important to maintain the temperature of the reaction vessel between -5°C – 0 °C. After HF had been removed, diethyl ether was added to the reaction mixture and the peptide-resin-scavenger mixture was stirred. The ether solution was filtered and the resin was washed three times to remove the scavengers. The peptide was extracted from the peptid-resin mixture by stirring the mixture in glacial acetic acid. This procedure was repeated twice to ensure complete extraction of the peptide, using approximately 30 cm^3 of 30 % acetic acid per gram of peptide-resin each time. The peptide solution was diluted with water to give a final concentration of AcOH less than 10% and lyophilized.

Solid-phase peptide synthesis using Fmoc strategy

Synthesis of the peptides by the Fmoc protocol were carried out on 2-chlorotrityl chloride resin. The Fmoc protocol is summarized in **Table 5**.

Step	Reagent	Time
Washing	DMF	3 × 1 min
Kaiser test		
Coupling	2 eq. Fmoc-amino acid 2 eq. HBTU and HOBt 4 eq. DIEA/DMF	30 min
Kaiser test		
Washing	DMF	3 × 1 min
Deprotection	20% piperidine/DMF	1 × 2 min and 1 × 20 min
Washing	DMF	3 × 1 min

Table 5. General schedule for peptide synthesis using Fmoc chemistry

After the last coupling step, the peptide-resin was washed with DMF and EtOH and then dried under vacuum. Final deprotection and cleavage from the resin was carried out by TFA in the presence of scavengers. The TFA cleavage reaction was performed at room temperature for 60 min, using the following mixture: 95% TFA, 2.5% water, 2.5% TIS. The peptide was precipitated by ice-cold diethyl ether, the peptide-resin mixture filtered-off, then the peptide was extracted by 10 % AcOH three times and finally lyophilized.

Purification of peptides

The crude peptides were purified by RP-HPLC on a semipreparative column (Vydac 218TP1010), applying gradient elution with the following eluents: A: 0.08% TFA/ACN, B: 0.1% TFA/water, flow rate was 4 cm^3/min, detected at 215 nm by UV detector.

Purity control was performed on a Merck-Hitachi or Merck-LaChrom RP-HPLC system, utilizing a Vydac 218TP54 C18 or Merck 50943 LiChroCART analytical column, with gradient elution. Detection was as described above. Peptide purity was assessed also by TLC on silica gel 60 F_{254}-precoated glass plates, the solvent systems were the following: (A) acetonitrile:methanol:water (4:1:1); (B) 1-butanol:acetic acid:water (4:1:1); (C) ethyl acetate:pyridine:acetic acid:water (60:20:6:11). Molecular weight of the peptides were determined by MALDI-TOF (Bruker Reflex III) or ESI-MS (Finnigan TSQ 7000 or Shimadzu QP 80000).

3.2. Tritium labeling of peptides

Before the radioactive labeling procedure the reaction was carried out in inactive circumstances, using hydrogen gas. This reaction helps to determine the proper reaction condition such as catalyst, reaction time, solvent.

The purified precursor peptide was dissolved in DMF and the catalyst ($PdO/BaSO_4$) was added. In most cases, an excess of TEA was added to neutralize HI formed during the reaction and to help prevent poisoning the catalyst. The reaction was carried out in hydrogen atmosphere at room temperature, while stirring continuously. The crude reaction mixture was analyzed by RP-HPLC and in some cases by MS.

Tritium labeling of peptides was carried out in our in-house designed vacuum apparatus (**10**) under a fume cupboard. The purified precursor peptide was dissolved in DMF and the catalyst was suspended in the solution. The reaction vessel was connected to the tritiation manifold frozen with liquid nitrogen and the air was removed by vacuum. The tritium gas was liberated from uranium tritide by heating above 300 °C, and it was expanded into the reaction vessel. The reaction mixture was agitated by the magnetic stirrer at room temperature. The reaction was terminated by freezing the solution and absorbing the unreacted tritium on pyrophoric uranium. The catalyst was removed by filtration through Whatman GF/C filters and washed three times with ethanol. Labile tritium was removed by repeated evaporation of protic solvent, such as $EtOH/H_2O$ mixture. The total activity of product was measured by LSC. The crude tritiated peptide was analyzed by TLC and RP-HPLC. The purified labeled peptide was dissolved in ethanol and stored in 2 cm^3 aliquots under liquid nitrogen at a radioactive concentration of 37 MBq/cm^3.

3.3. Characterization of tritiated peptides

Determination of specific activity

The specific activity of the labeled peptides was determined by dividing the measured activity by the amount of purified peptide. The quantity of the purified labeled material was determined from its UV absorption spectrum, or by HPLC, using calibration curve.

Tritium distributions in labeled peptides

The labeled peptide was diluted by inactive material, 6M HCl was added, and the mixture was incubated at 110 °C for 24 h under argon pressure in a sealed ampoule. The solvent was then removed by evaporation. The formed amino acid mixture was analyzed by TLC and subsequently to the formation of the Fmoc derivatives by RP-HPLC. Fmoc derivates of amino acids were used as standards respectively (**144**).

The sample - amino acid or peptide hydrolysate - was dissolved in borate buffer (0.2 M, pH: 7.7). Fmoc-Cl reagent was dissolved in aceton to give a concentration of 15 mM. The sample and the reagent were mixed, and after 45 seconds the vial was filled with n-pentane and the mixture was shaken to remove the excess reagent. The extraction was repeated twice

and the pentane phases were discarded. Afterwards the sample had been acidified 10 µl of acetic acid and then analyzed by RP-HPLC (**145**).

3.4. Methods for investigation of the metabolism of tritiated peptides

After preincubation of the rat brain homogenate, tritium labeled peptides were incubated with it at 37 °C. Aliquots were withdrawn after incubation for 5, 15, 30 or 60 min, and immediately acidified with 0.1 M HCl solution. Following centrifugation of the samples (11,340 × g, 5 min, 25 °C) and the supernatant was analysed by radio-HPLC. For determination of the rates of degradation of the peptides the following method was applied. Aliquots of the 1 mM nonlabeled peptide stock solutions in 50 mM Tris–HCl buffer (pH = 7.4) were added to some rat brain homogenate, and the mixtures were incubated at 37 °C. Aliquots were taken from these incubation mixtures and immediately acidified with 0.1 M aqueous HCl solution. About 10 µl of each supernatant obtained after centrifugation of the samples (11,340 × g, 5 min, 25 °C) was analysed by RP-HPLC. The degradation rate constants (k) were obtained by least square linear regression analysis of the plots of logarithmic peptide peak areas ($\ln(A/A_0)$) versus time, using a minimum of four points. Degradation half-lives ($t_{1/2}$) were calculated from the rate constants as ln(2/k).

3.5. Peptide isolation methods from rat brain

Animals

Animal care and experimental procedures were carried out according to the principles set by EC Directive 86/609/EEC. Experimental protocols were approved also by the Ethical Board controlling laboratory experiments at the Medical Faculty of Semmelweis University. Male Wistar rats, weighing 110–150 g (analgesic measurements) or 170–220 g (brain extracts), were used. Rats were kept in groups of 5, in temperature-controlled (22 ± 2 °C) unit with 12 h light–dark cycle (08.00–20.00–08.00). Standard laboratory chow and tap water were provided ad libitum.

Peptide-extraction procedures from rat brain

Rat brains were removed and powderized under liquid nitrogen, taken up with abs. ethanol and stored at -80 °C until extraction. An extraction procedure deviced originally for endomorphins (**59**), was used, except for sample boiling. In brief, the stored samples were solubilized in eight-fold amount of 0.08% (w/w) $Na_2S_2O_5$ solution then ACN was added to yield 25% (v/v) final ACN concentration. They were mixed at room temperature overnight. The mixtures were centrifuged at 29,000 × g for 20 min and the supernatants were extracted by solid-phase method , using 70% (v/v) ACN in the final step. The extracts were evaporated

to dryness and dissolved in 2% ACN/ 98% water (TFA 0.1% (v/v)) and the samples were analyzed by RP-HPLC. Chromatographic conditions were the following: Vydac 218TP54 C18 reverse-phase column (250 × 4.6 mm, 5 μm) at a flow rate of 1 cm^3/min at ambient temperature. The mobile phase was mixed from 0.1% (v/v) TFA in water and 0.08% (v/v) TFA in ACN, and gradient elution was carried out from 2% to 40% of ACN within 30 min.

^{125}I-labeling of peptides containing tyrosine

RIA is based on the antigen-antibody reaction in which tracer amount of the radio-labeled antigen competes with endogenous antigen for limited binding sites of the specific antibody against the same antigen. Usually, high specific activity radio-labeled antigen is prepared by iodination of the pure antigen on its tyrosine residue(s) by chloramine-T (**146**) method and then separating the radio-labeled antigen from free-isotope by gel-filtration or HPLC. The lyophilized peptide was dissolved in phosphate buffer (pH = 7.4). Iodinations was performed by addition of chloramine-T solution to a polypropylene tube containing a mixture of 1v/v% TFA solution, peptide and $Na^{125}I$ (in 0.04M NaOH) solution. The iodination reaction was quenched after 1 min by addition sodium metabisulphite in water. ^{125}I-peptide was immediately purified by RP-HPLC. The fractions were collected at 12-sec intervalls. The radioactivies in the peak fraction were measured by counting 2 μl aliquots on a LIN-LOG NK-350 gamma counter and the radioactivities of the pure, collected ^{125}I-EM2 were measured by a TRI-CARB 2100TR liquid scintillation counter in a toulene-Triton X-100 cocktail. An aliquot of the peak radioactive fraction was then rechromatrographed as above in the presence of 5 nmol of unlabeled EM2 while simultaneously monitoring UV absorbance at 216 nm and gamma emissions by using Canberra Packard Radiomatic 505TR Flow Radiochromatography Detector with the Ultima-FloM scintillation cocktail.

Preparation of endomorphin 2-keyhole limpet hemocyanin conjugate

Based on an earlier method (**147**)**,** approximately 10 mg of keyhole limpet hemocyanin and 5 mg of endomorphin 2 were dissolved together in 10 cm^3 of water. To this mixture was added 0.5 cm^3 of water containing 100 mg of freshly dissolved water soluble carbodiimide reagent and it was incubated overnight at room temperature. The unadjusted pH of the reaction mixture was 5–6. The reaction was terminated by dialysis against water for 24 h. When precipitates formed, the granular and soluble materials were used together for immunization.

3.6. Tc-99m-labeling of annexin V fragments via nitrido intermediate

Stability studies

Before the labeling, a long run stability studies of the solid, non-radiolabeled Anx13 were carried out by storing them at –18 ^{o}C and at +5 ^{o}C. For short time heat tolerance investigations, the aqueous/saline solution of the Cys-Cys-Anx13 were used by immersing them into boiling water for 20 and 60 minutes.

Synthesis of $[^{99m}Tc \equiv N]^{2+}$ intermediate

Nitrido intermedier was prepared at ambient temperature by using succinic acid dihydrazide (SDH), $SnCl_2$ in saline and freshly eluted $^{99m}TcO_4^-$ (37-185 MBq). The mixture was stirred at room temperature for 15 min.

Labeling of peptides via nitrido intermediate

Symmetric nitrido labeling were carried out by adding peptide in saline to the ^{99m}Tc-nitrido intermediate. The reaction mixtures were heated in boiling water bath for 1 hour. For asymmetric labeling peptide in saline, bis(dimethoxypropyl-phosphinoethyl) methoxyethylamine (PNP) in ethanol or tris(2-cynoethyl)phosphine (PCN) in hydroxypropyl-γ-cyclodextrin was reacted with the previously prepared ^{99m}Tc-nitrido intermediate at 100 ^{o}C for 1 hour.

Determination of the radiochemical purity

Radiochemical purity of the nitrido labeled peptides was determined by HPLC and TLC methods. For HPLC, Zorbax 300 SB C-18 column with both radioactivity and UV detectors were used. Solutions A and B were prepared for gradient elution containing 0.1 % TFA in water and 0.08% TFA in ACN, respectively. TLC was carried out by using Kieselgel 60 layers and ethanol-water 1:1 (v/v) as eluent or Gelman ITLC-SA leyers and n-buthanol saturated with 0.3M HCl solution as eluent. For determination of free pertechnetate content, Whatman ET-31 paper and acetone eluent were also used.

4. Results and Discussion

4.1. Synthesis and tritiation of endomorphin analogues

Dmt[1]-endomorphin 2

Synthesis

Peptides (H-Dmt-Pro-Phe-Phe-NH_2 and H-Dmt-$^{3,4}\Delta$Pro-Phe-Phe-NH_2 precursor peptide) were synthetized manually on MBHA resin in 0.25 mmol scale by using the Merrifield solid-phase method. N^{α}-t-Boc chemistry with HOBt and DCC as coupling agents were employed for peptide elongation. The crude peptides were purified by RP-HPLC on a Vydac 218TP1010 C18 column, using a linear gradient of from 20% to 50% of the organic modifier within 25 min at a flow rate of 4 cm^3/min with UV detection at 220 nm. Peptide purity was assessed by TLC and HPLC, and the molecular weights of the peptides were established by MALDI-TOF-MS. R_f values, capacity factor for a Vydac 218TP54 C18 column and the measured and calculated molecular weights of Dmt-EM2 analogues show in the **Table 6**. R_f values were establish on silica gel 60 F_{254}-precoated glass plates. The solvent systems were following: (A) acetonitrile:methanol:water (4:1:1), (B) 1-butanol:acetic acid:water (4:1:1), (C) ethyl acetate:pyridine:acetic acid:water (60:20:6:11).

Peptides	**TLC**			**HPLC**	**MS**	
	R_f (A)	R_f (B)	R_f (C)	k'	$[M+H]^+$	Mr
Dmt-Pro-Phe-Phe-NH_2	0.36	0.53	0.33	3.04	600.37	599
Dmt-ΔPro-Phe-Phe-NH_2	0.39	0.53	0.33	3.01	598.33	597
Diiodo-Dmt-Pro-Phe-Phe-NH_2	0.50	0.57	0.43	5.91	852.24	851

Table 6. Analytical data of Dmt-EM2 analogues

A precursore peptide, 3`, 5`-Diiodo-Dmt[1]-EM2 was synthetized by the chloramine T method. Testing was performed to establish the optimum reaction conditions. Accordingly, 1.4 μmol of Dmt[1]-EM2 was dissolved in acetonitrile:water (1:1) and 5 equivalents of the reagents (0.067 M NaI + 0.022 M chloramine T in phosphate buffer, pH = 7.4) was added to the solution. The reaction was stopped after 30s by adding 0.053 M $Na_2S_2O_5$. The reaction mixture was analysed and purified by RP-HPLC (Vydac 218TP54 C18 RP column with a gradient of 20% to 50% of organic modifier in 25 min, flow rate 1 cm^3/min). The analytical parameters of Diiodo-Dmt[1]-EM2 show in the **Table 6.**

Tritiation

2.4 mg (2.88 μmol) of 3`,5`-diiodo-Dmt[1]-EM2 and 2.8 mg (3.92 μmol) of $^{3,4}\Delta Pro^2$-Dmt[1]-EM2 were dissolved separately in 1 cm^3 of dimethylformamide and labeled with tritium gas. The reaction mixture contained 1.5 μl of triethylamine and 12 or 14 mg of PdO/$BaSO_4$ catalyst, respectively. Tritium gas was liberated from uranium tritide by heating, and 555 GBq

(15 Ci) of this gas was introduced into the reaction vessel (**10,79**). The reaction mixture was stirred at room temperature for 1 or 2 h and the unreacted tritium gas was then adsorbed onto pyrophoric uranium. The crude products were purified by HPLC to give a radioactive purity of >95%. The quantitative analysis of the pure, labeled peptides was performed by HPLC with a UV detector, using a calibration curve prepared with unlabeled Dmt^1-EM2, and the total activities of the products were measured by liquid scintillation counting. The specific activity of [$^3H_2$]-Dmt^1-EM2 were 2.88 TBq/mmol (77.8 Ci/mmol), and that of [$^3H_2$]Pro-Dmt^1-EM2 1.95 TBq/mmol (52.8 Ci/mmol) (**Table 7**). The pure, tritiated peptides were dissolved in ethanol and were stored at a concentration of 37 MBq/cm^3 under liquid nitrogen. The stabilities of both tritiated endomorphin 2 analogues under these storage conditions were really good. After 6 months, the purities were checked and proved to be >95%.

Peptides	a TBq/mmol	TLC			HPLC k'
		R_f (A)	R_f (B)	R_f (C)	
[3',5'-$^3H_2$]Dmt-Pro-Phe-Phe-NH_2	2.88	0.36	0.53	0.33	3.26
Dmt-[3,4-$^3H_2$]Pro-Phe-Phe-NH_2	1.95	0.36	0.53	0.33	3.26

Table 7. Radioanalytical data of tritium labeled Dmt-EM2

Distribution

The distributions of the tritium labels in [$^3H_2$]Dmt^1-EM2 and [$^3H_2$]Pro^2-Dmt^1-EM2 were determined after acidic hydrolysis and Fmoc derivatization by HPLC. The Dmt and Pro contained tritium in >90% of the theoretical level. The a/amax is the ratio of the specific to the theoretically maximum specific activity. The Phe residues in the peptides were also partially labeled (**Table 8**). This phenomenon presumably caused the overall higher specific activity of [$^3H_2$]Dmt^1-EM2 than the theoretical level. The specific activity of [$^3H_2$]Pro^2-Dmt^1-EM2 was >90 % of theoretical level, and the specificity of the label was satisfactory, resulting in an appropriate radioligand for radioligand-binding experiments and metabolic studies.

Tritiated peptides	a/a_{max}	HPLC		
		Fmoc-[$^3H_2$]Dmt	Fmoc-[$^3H_2$]Pro	Fmoc-[^{3}H]Phe
[$^3H_2$]Dmt^1-EM2	133%	92%	-	8%
Dmt-[$^3H_2$]Pro^2-EM2	92%	1%	95%	4%

Table 8. Tritium distributions in Dmt-EMs

Stability

The stability of a radioligand in radioligand-binding studies is essential, and it is therefore necessary to determine the degradation half-life of the ligand in the biological matrix used. In our earlier investigations, EM1 and EM2 demonstrated long half-lives in the

presence of a rat brain membrane preparation (0.3 mg/cm^3 protein): 295 min and 230 min, respectively, accordingly they do not degrade during binding assays (**148**). In the present study, the degradation half-life of [$^3H_2$]Pro^2-Dmt^1-EM2 under the above conditions was 515 min. The kinetics of degradation of Dmt^1-EM2 was studied in a rat brain homogenate, as compared with the earlier published degradation kinetics of EM2 (**79**). The protein content of the homogenate was 5.92 mg/cm^3 and Dmt^1-EM2 concentration was 100 μM. **Figure 2.** shows the kinetics of degradation of EM2 and Dmt^1-EM2 in the rat brain homogenate. After 12 min of incubation, only 24% of the parent EM2 remained in the samples, whereas 72% of the initial Dmt^1-EM2 concentration remained after 15 min of incubation.

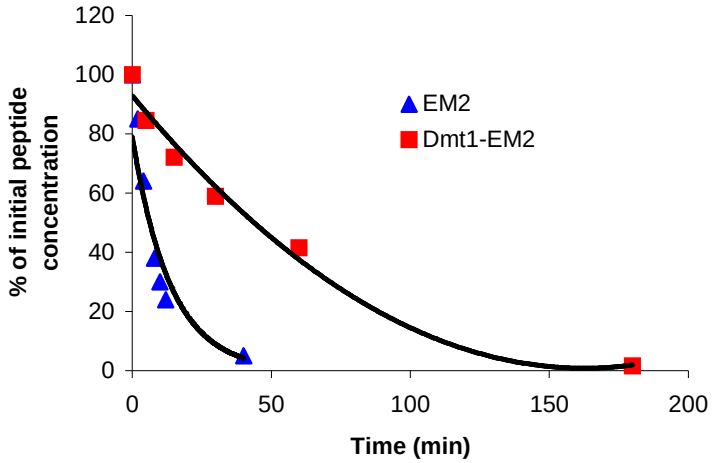

Figure 2. Degradation of EM2 and Dmt^1-EM2 in rat brain homogenate

The logarithmic forms of these curves were analysed by linear regression, which allowed calculation of the degradation half-lives of the EMs. As shown in **Table 9**, Dmt^1-EM2 broke down relatively slowly in the brain homogenate. Dmt^1-EM2 had a half-life of 33.64 min, while EM2 was almost 6 times less resistant than Dmt^1-EM2 to the peptidases: its half-life was 5.88 min.

EM2		**Dmt^1-EM2**	
100 x k (min^{-1})	**$t_{1/2}$ (min)**	**100 x k (min^{-1})**	**$t_{1/2}$ (min)**
11.79 ± 0.75	5.88 ± 0.39	2.09 ± 0.39	33.64 ± 6.81

Table 9. Half-lives of EMs

4.2. Synthesis and tritiation of peptide analogues from Zebrafish

Synthesis

The endogenous MEGY, (H-Tyr-Gly-Gly-Phe-Met-Gly-Tyr-OH) its two analogs, (D-Ala^2)-MEGY and (D-Ala^2, Val^5)-MEGY, and the precursor peptide for tritiation (3`, 5`-Diiodo-Tyr^1-MEGY) were synthesized by the above-mentioned solid-phase peptide synthesis method using the Boc chemistry procedure. The crude peptides were purified by RP-HPLC using a Vydac 218TP1010 column. Peptide purity was assessed by TLC and RP-HPLC, and the molecular weights of the peptides were established by MALDI-TOF-MS. R_f values, capacity factor for a Vydac 218TP54 C18 column and the measured and calculated molecular weights of Dmt-EM2 analogues show in the **Table 10.** R_f values were establish on silica gel 60 F_{254}-precoated glass plates. The solvent systems were following: (A) acetonitrile:methanol:water (4:1:1), (B) 1-butanol:acetic acid:water (2:1:1), (C) ethyl acetate:pyridine:acetic acid:water (60:20:6:11).

Peptides	TLC			HPLC	MS	
	R_f (A)	R_f (B)	R_f (C)	k'	$[M+H]^+$	Mr
Tyr-Gly-Gly-Phe-Met-Gly-Tyr	0.63	0.62	0.14	2.06	794.25	793
Tyr-D-Ala-Gly-Phe-Met-Gly-Tyr	0.70	0.68	0.21	2.27	808.37	807
Tyr-D-Ala-Gly-Phe-Val-Gly-Tyr	0.60	0.68	0.14	1.75	776.31	775

Table 10. Analytical data of MEGY analogues

Tritiation

[3',5'-$^3H_2$]MEGY was prepared by catalytic dehalogenation of the precursor peptide using 555 GBq (15 Ci) $^3H_2$ gas and 11.5 mg $PdO/BaSO_4$ as the catalyst in the presence of triethylamine. The crude tritiated peptide was purified by RP-HPLC as previously described. The purity of the final product was established by analytical RP-HPLC and the degree of purity observed was >95%. The total activity of the product was 3.51 GBq (95 mCi). The specific radioactivity was 0.74 TBq/mmol (20 Ci/mmol). The purified peptide was stored in ethanol under liquid nitrogen at a concentration of 37 MBq/cm^3 (1 mCi/cm^3).

Saturation binding assays

The ability of [^{3}H]MEGY to bind opioid receptors from zebrafish, an organism in which this peptide is naturally present (**149**), and from mammals, in which MERF is the corresponding endogenous peptide, was measured using increasing concentrations of this radioligand in zebrafish and rat brain membrane homogenates.

In zebrafish brain K_D was 2.39 ± 0.29 nM and B_{max} was 255.1 ± 10.84 fmol/ mg protein. The same analysis is presented for rat brain membranes, K_D was 3.8 ± 0.34 nM and B_{max} was 308.1 ± 11.45 fmol/mg protein. MEGY can bind to the opioid receptors present in zebrafish

and rat brain with high affinity and that this binding is reversed by naloxone. The binding assays of [^{3}H]MEGY obtained by us give similar saturation curves for zebrafish and rat brain homogenates, although this peptide presents a significant higher affinity in zebrafish brain (Results from Dr. Raquelle Rodriguez's team).

Results and discussion of competition binding assays

To analyze the ability of MEGY to displace other conventional opioid compounds, competition binding assays were performed using [^{3}H]diprenorphine, a nonspecific antagonist, as the radioligand and MEGY and its two analogs, (D-Ala^2)-MEGY and (D-Ala^2, Val^5)-MEGY, as unlabeled ligands at a concentration range of 0.3 nM to 10 μM (Results from Dr. Raquelle Rodriguez's team).

Ligand	**K_i Zebrafish Brain / nM**	**Displacement in Zebrafish Brain %**	**K_i Rat Brain / nM**	**Displacement in Rat Brain %**
MEGY	K_{i1} = 1.17 ± 0.27 K_{i2} = 673 ± 136	74.28 ± 4.20	22.10 ± 1.57	72.20 ± 7.15
(D-Ala^2)-MEGY	12.40 ± 2.67	63.89 ± 2.69	29.90 ± 7.97	85.45 ± 2.23
(D-Ala^2,Val^5)-MEGY	137 ± 26.45	54.64 ± 2.36	72.20 ± 7.15	79.39 ± 3.30

Table 11. K_i values of MEGY and its two analogs in zebrafish and rat brain membranes obtained from competition binding assays using [^{3}H]diprenorphine

[^{3}H]diprenorphine presents two different binding sites in zebrafish brain (K_D values 0.08 and 17 nM) (**150**), and in the further assays, MEGY shows a two-site displacement in zebrafish brain, with high-affinity site and one site with lower affinity, which suggests that this peptide may act on two or more different receptors with different affinities. Preliminary work from R. E. Rodriguez's laboratory proposes that MEGY binds to the δ receptors from zebrafish (**150**).

The fact that a ligand shows a biphasic curve in competition binding assays has been previously reported for other ligands, such as morphiceptin (**151**).

In the rat, the analog (D-Ala^2)-MEGY shows a similar K_i and percentage of displacement at 10 μM than MEGY, thus indicating that the change of Gly by a D-Ala does not affect the ability of the ligand to bind to opioid sites. However, the (D-Ala^2, Val^5)-MEGY analog displays a higher K_i, revealing that the change of Met by Val entails a loss in binding affinity. These results can be taken into consideration for future opioid ligand design because an effective peptidic ligand should have the methionine in the fifth position, whereas the Gly can be replaced by another small residue that might confer resistance against protease degradation.

MEGY and its two analogs can displace almost all the diprenorphine binding in rat brain, whereas in zebrafish brain, the native peptide displaces only up to 74%. This difference can be explained if we postulate that diprenorphine may bind to the opioid sites present in zebrafish brain in a different manner than to those present in mammalian brain. These results are interesting because it may be inferred that diprenorphine can be considered as a good and selective ligand to label opioid sites in mammalian brain, whereas in zebrafish diprenorphine does not seem to show such selectivity and thus, other opioid ligands are not able to displace up to 100% of its binding.

[^{3}H]MEGY was also used as the radioligand in competition binding assays using the unlabeled peptide MEGY and its two analogs as unlabeled ligands so that it was possible to determine the influence of the structural changes in the binding ability. Heterologous displacements with morphine (nonpeptidic opiate) and Met-enkephalin (an endogenous ligand for both species) were also performed (**Table 12.**)

Ligand	**K_i Zebrafish Brain / nM**	**Displacement in Zebrafish Brain %**	**K_i Rat Brain / nM**	**Displacement in Rat Brain %**
MEGY	2.89 ± 0.85	106.85 ± 1.40	4.21 ± 1.41	109.51 ± 1.19
(D-Ala^2)-MEGY	7.65 ± 1.99	112.72 ± 4.90	4.45 ± 1.21	100.16 ± 1.48
(D-Ala^2,Val^5)-MEGY	25.93 ± 3.47	110.25 ± 2.46	21.06 ± 2.71	100.15 ± 0.92
Met-enkephalin	2.01 ± 0.59	108.43 ± 1.65	2.40 ± 0.29	102.55 ± 1.06
Morphine	14.15 ± 2.61	114.12 ± 2.69	7.23 ± 1.57	97.44 ± 3.78

Table 12. K_i values of several ligands in zebrafish and rat brain membranes obtained from competition binding assays using [^{3}H]MEGY

In case of (D-Ala^2,Val^5)-MEGY, the changes in the peptide structure showed decreased values in binding affinity in zebrafish brain. However, in rat brain, the substitution of Gly by a D-Ala does not entail a change in the inhibition constant K_i, probably because this modification does not cause a change in size or in charge of the ligand. Met-enkephalin shows a similar pattern to the one observed for MEGY in zebrafish brain, whereas in rat brain it displays a lower K_i value, possibly because it is an endogenous ligand for mammalian opioid receptors, although to our knowledge the MEGY peptide is not naturally present in tetrapods. All the ligands studied are able to present a higher displacement than naloxone, especially when acting on zebrafish brain. This observation can be explained if we consider that the [^{3}H]MEGY peptide, apart from binding to naloxone-sensitive opioid sites, also binds to some sites that are not recognized by naloxone. Sites recognized by naloxone should be considered as classical opioid sites, and the naloxone-insensitive sites should be named as nonclassical opioid sites. Therefore, the expression “nonopioid” could be used accurately when an opioid

ligand acts on a different receptor than the opioid receptors (e.g., the Met-enkephalin and its derivatives on the cytosolic opioid growth factor receptor) (**152**).

Present data point to the possibility that the antagonist naloxone does not bind to some sites that are recognized by the agonists; hence, the MEGY peptide presents a higher selectivity for recognizing the opioid binding sites in zebrafish. In conclusion, these results prove that the MEGY peptide acts as a highly specific endogenous ligand for the zebrafish opioid receptors and also binds with high affinity to their mammalian counterparts. Our work reveals that the zebrafish opioid peptide MEGY presents a different binding profile than other opioid agonists; therefore, this ligand can be used as a new tool to investigate the ligand-receptor in- teractions in relation to the modulation of pain and drug addiction.

4.3. Investigation of a possible endomorphin biosynthesis route

Synthesis

Peptide amides (endomorphin 1 and 2) were prepared on MBHA resin, and peptide acids (YP, 3',5'I_2-YP, YPW, YPF, YPWF, YPFF) in 0.25 mmol scale on choromethylated resin (Merrifield resin). The crude peptides were purified by RP-HPLC on a Vydac 218TP1010 C18 column, using a linear gradient from 5% to 50% of the organic modifier (ACN) within 30 min at a flow rate of 4 cm^3/min, with UV detection at 220 nm. The purities of peptides were assessed by TLC and analytical HPLC. The molecular weights of the peptides were confirmed by ESI-MS or MALDI-TOF-MS. R_f values were establish on silica gel 60 F_{254}-precoated glass plates. The solvent systems were following: (A) acetonitrile:methanol:water (4:1:1), (B) 1-butanol:acetic acid:water (4:1:1), (C) ethyl acetate:pyridine:acetic acid:water (60:20:6:11). (**Table 13.**).

Peptides	**TLC**			**HPLC**	**MS**	
	R_f (A)	**R_f (B)**	**R_f (C)**	**k'**	**$[M+H]^+$**	**Mr**
Tyr-Pro	0.41	0.44	0.13	1.05	279.17	278
H-Diiodo-Tyr-Pro	0.48	0.48	0.28	2.89	530.92	529.8
Tyr-Pro-Phe	0.44	0.47	0.31	2.70	426.40	425
Tyr-Pro-Trp	0.45	0.47	0.27	3.07	465.40	464
Tyr-Pro-Phe-Phe	0.53	0.54	0.33	4.43	573.60	572
Tyr-Pro-Trp-Phe	0.53	0.53	0.32	4.72	612.40	611
Tyr-Pro-Trp-Phe-NH_2	0.45	0.56	0.34	4.26	611.60	610
Tyr-Pro-Phe-Phe-NH_2	0.43	0.55	0.37	3.94	572.70	571

Table 13. Analytical data of EM fragments

Tritiation

2.0 mg (3.76 μmol) of precursor peptide dissolved in 1 cm^3 of DMF was tritiated with tritium gas using tritium manifold. The reaction mixture contained 1.5 μl triethylamine and 12.2 mg $PdO/BaSO_4$ catalyst. Tritium gas was liberated from uranium tritide by heating, and 555 GBq (15 Ci) of it was introduced into the reaction vessel. The crude product was purified by RP-HPLC to give a radioactive purity of >95%, The total activity of the product was 4.44 GBq (120 mCi). The calculated specific activity was 1.85 TBq/mmol (49.9 Ci/mmol).

Results of the chromatographic procedure

In our experimental composition two series were designed. In the first series twelve animals (1.1–1.12) were sacrificed, four at 15, four at 30 and the last four at 60 min after 0.74 MBq (20 μCi) of [$^3H_2$]Tyr-Pro intracerebroventricular (*icv*) injection. In the second series, only four animals (2.1–2.4) were treated with 7.4 MBq (200 μCi) of [$^3H_2$]Tyr-Pro, all sacrificed at 30 min. After the extraction procedures, RP-HPLC analysis of purified rat brain extracts was carried out. Radiodetection (upper parts in panels A, B, C, D) and UV (at 220 nm) detection (lower parts in panels A, B, C, D) were used. In the UV chromatograms the co-injected standards appear with the exact retention times.

The UV chromatographic profile of co-injected standard mixture outlined three regions. In the first region appear Tyr and YP (around 8 and 11 min, respectively), in the second YPF and YPW tripeptides (around 18 min) and the tetrapeptide cluster from 19.5 min, the order of retention times being YPFF-NH_2<YPFF-OH<YPWF-NH_2<YPWF-OH.

In the ‘‘20 μCi’’ series, at 15 min, a radioactive peak corresponding to Tyr appeared in all the three samples, both Tyr and YP in one (No. 1.2) and none in the tri- and tetrapeptide region **(Fig. 3.,** panel A). At 30 min, in two samples only minor active peaks at the position of Tyr were found, and none in the other two regions. In extract No. 1.6, besides YP, YPFF-OH could also be identified among the active peaks (**Fig. 3.**, panel C). In one sample (No. 1.5), besides Tyr, one peak which could be identified as YPFF-OH and one additional peak in the tripeptide region, possibly YPF, appeared in the radiochromatogram (**Fig. 3.**, panel B). Apart from a minor active Tyr peak in one of four extracts, no activity could be detected in extracts at 60 min (not shown). In the ‘‘200 μCi’’ series, although peaks appeared both in the tri- and tetrapeptide regions in all samples, only one robust peak could be identified with safety as YPFF-NH_2 in sample No. 2.4 (**Fig. 3.**, panel D).

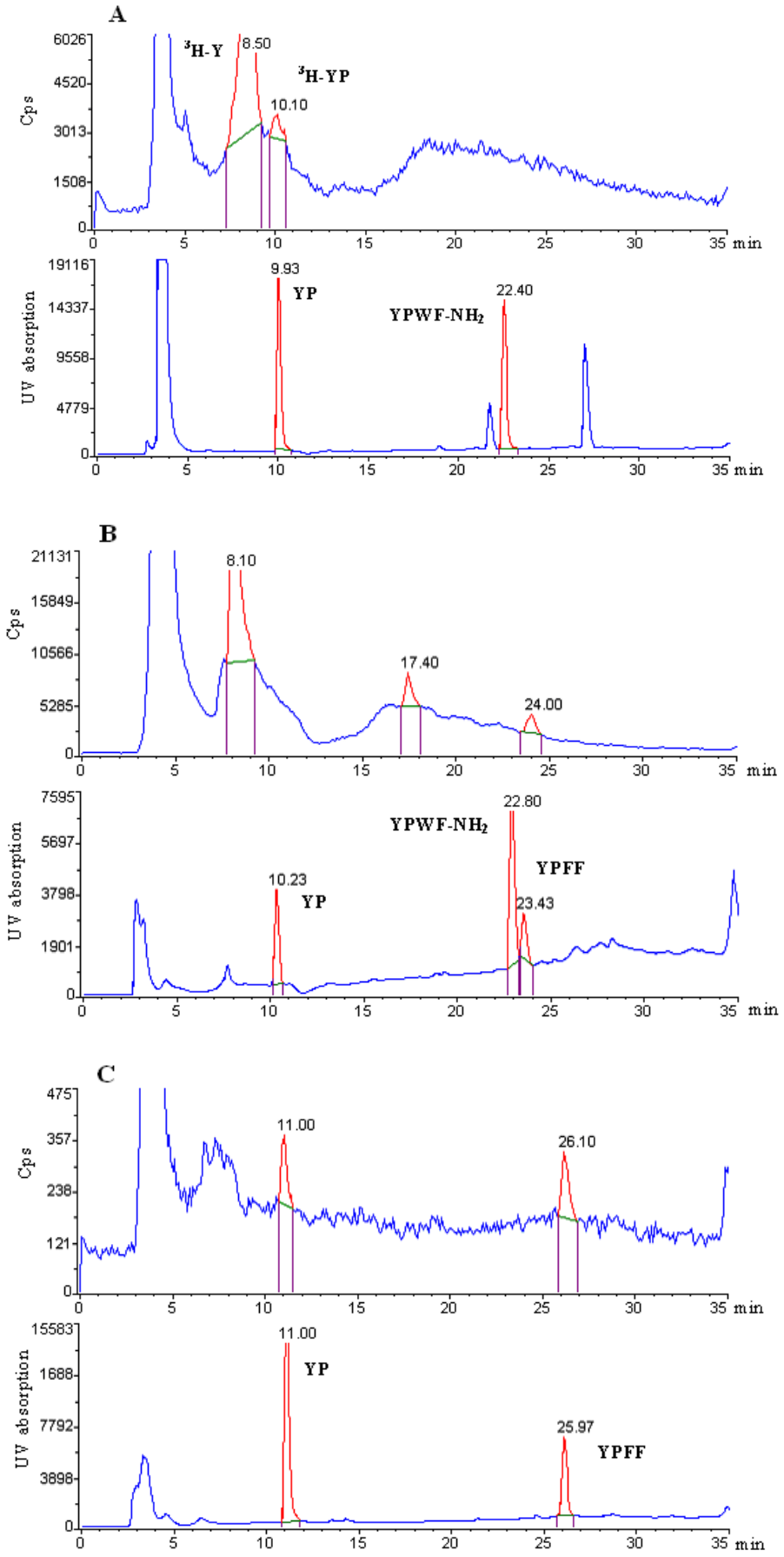
A
Cps
6026
4520
3013
1508
0
^{3}H-Y
8.50
^{3}H-YP
10.10
0 5 10 15 20 25 30 35 min
UV absorption
19116
14337
9558
4779
0
9.93
YP
22.40
YPWF-NH$_2$
0 5 10 15 20 25 30 35 min
B
Cps
21131
15849
10566
5285
0
8.10
17.40
24.00
0 5 10 15 20 25 30 35 min
UV absorption
7595
5697
3798
1901
0
22.80
YPWF-NH$_2$
YPFF
10.23
YP
23.43
0 5 10 15 20 25 30 35 min
C
Cps
475
357
238
121
0
11.00
26.10
0 5 10 15 20 25 30 35 min
UV absorption
15583
1688
7792
3898
0
11.00
YP
25.97
YPFF
0 5 10 15 20 25 30 35 min

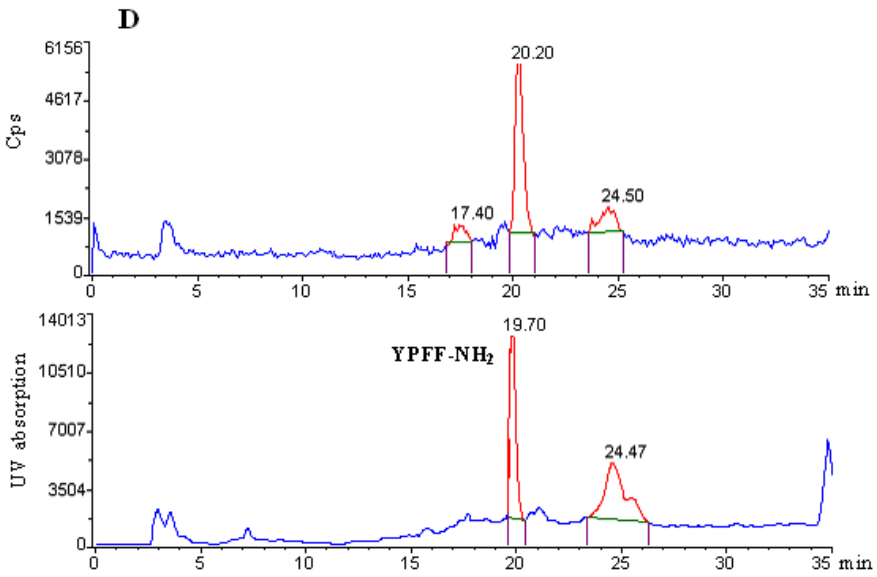

Figure 3. RP-HPLC analysis with online radiodetection of processed brain extracts obtained from rats injected *icv* with 0.74 MBq (panel A, B, C) or 7.4 MBq of [$^{3}H_2$]-Tyr-Pro (panel D)

Synthesis of ^{125}I-endomorphin 2

The lyophilized EM2 was dissolved to a final concentration of 1.46 mM in 25 mM sodium phosphate buffer (pH =7.4). Iodinations was performed by addition of 20 µl of a 0.25 mg/cm^3 solution of Chloramine T to a polypropylene tube containing a mixture of 50 µl of 1v/v% trifluoroacetic acid solution, 7.3 nmol of EM2 and 37 MBq (1 mCi) of Na^{125}I. The iodination reaction was stopped after 1 min by addition of 20 µl of 0.5 mg/cm^3 sodium metabisulphite in water. The total activity of the pure labeled peptide was 16.83 MBq (455 µCi). The specific activity was approximately 72 TBq/mmol (2000 Ci/mmol).

Results of the radioimminoassay

Six male rabbits received a primary dosing and 3–6 booster injections of EM2-hemocyanin conjugate. From the first booster, 14–16 days after the injection blood was drawn and antibody production was determined. From the third booster, treatment was continued in three rabbits (R1, R2 and R4). Antisera raised in R1 and R4 were used for further experimentation.

R1 antiserum recognized EM2 with a median sensitivity of 65.5± 7.5 pg/tube (n=7), and did not recognize EM1 even at 500 pg/tube. R4 antiserum recognized EM1 with a median sensitivity of 113.5 ± 26,7 pg/tube (n=8) and also EM2 (46.3±11.3% (n=4) displacement at 500 pg/tube, although the displacement curve for the latter was rather shallow.

Neither antisera recognized N-terminal di- and tripeptide endomorphin fragments or endomorphins with a free C-terminal carboxylic function (i.e. EM1-OH and EM2-OH, resp), or reacted with [Met^5]- or [Leu^5]-enkephalins, [Met^5]-enkephalin-Arg^6,Phe^7, β-endorphin or [D-Ala^2]-dynorphin-A(1–17). Using endomorphin antisera in purified rat brain extracts, EM2-like immunoreactivities were found in the RP-HPLC gradient-separated fractions corresponding to the retention time of standard EM2 but also in the fraction at the retention time of EM2-OH standard (a representative scale-matched run is shown in **Fig. 4.**).

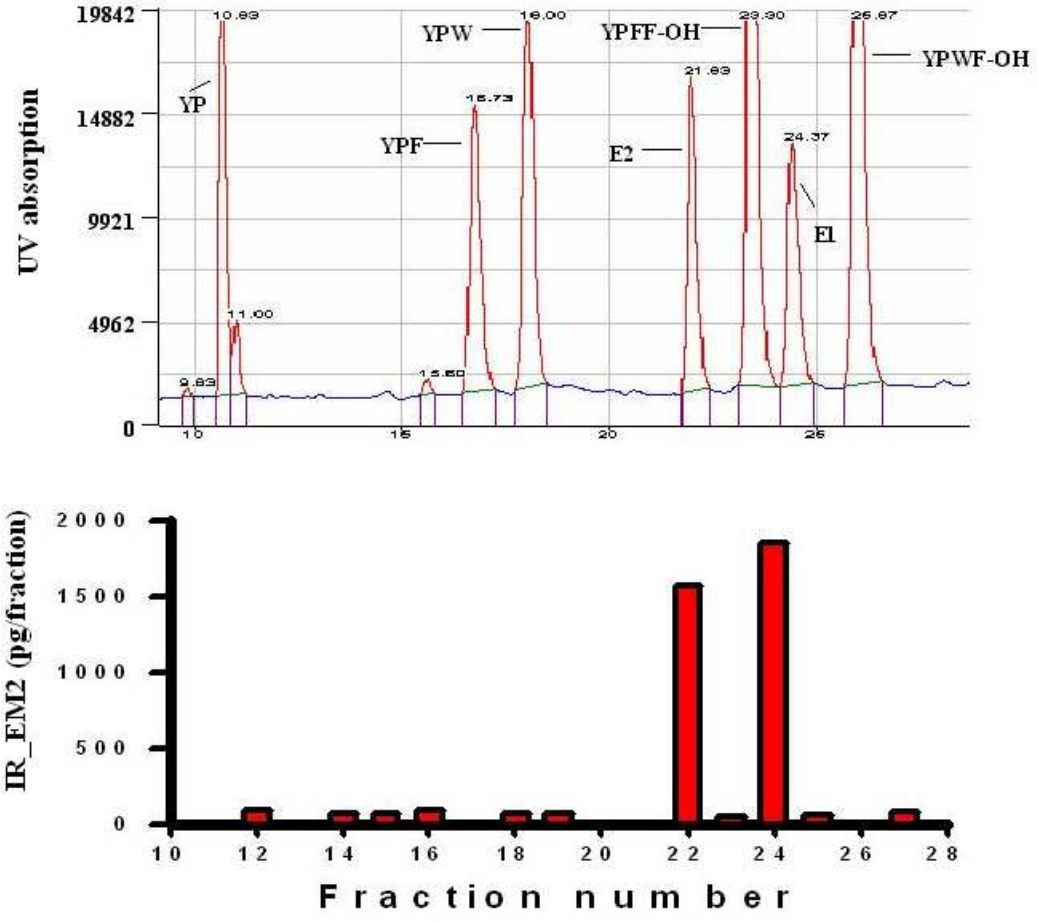

Figure 4. Endomorphin 2-like immunoreactivities found in RP-HPLC gradient separates of rat brain extract. (R1 antiserum) The scales of panels were matched so that immunoreactivity at "22" represents peptide(s) with retention time(s) between 21–22 min etc.

The EM2-like immunoreactivity found in the authentic EM2 fraction was 144.6±40.0 pg/g and 179.1±30.1 pg/g (n=3) in the fraction matching EM2-OH standard. Since R1 does not recognize authentic EM2-OH, the immunoreactive substance must be a different entity. R4 antiserum, due to its cross-reactivity, also recognized EM2-like immunoreactivities in brain extracts with similar sensitivity. We have failed to establish the structural identity of

novel immunoreactive species by MS for technical reasons. Furthermore, we did not detect immunoreactivities by R4 antiserum in the region where EM1-related standards appeared in the chromatogram.

Discussion of the investigation of a possible endomorphin biosynthetic route

According to doctrine, endogenous peptides should be generated from large molecular weight precursors by post-translational processing (**141**). In this case, appearance of labeled tyrosine in the end-products would entail first the hydrolysis of [^{3}H]Tyr-Pro dipeptide to yield [^{3}H]Tyr, the ribosomal incorporation of labeled Tyr into precursor, followed by processing. Unless the time course of presumed, still unidentified endomorphin precursor production and post-translational processing is entirely different from the ones described e.g. for pro-opiomelanocortin, insulin- or parathyroid hormone precursors/end-products (**153-156**), the presently found time course of incorporation of label into endomorphin 2-related tetrapeptides rules out the route via precursor generation and processing. As it was stated, ‘‘labeled amino acids do not begin to appear in the final products of biosynthetic pathway until about 45 min after the beginning of labeling” (**154**). In our experiments, incorporation of label into endomorphin 2-related tetrapeptides was found in brain extracts at 30 but not 60 min after *icv* injection of ^{3}H-Tyr-Pro. The time course of tyrosine generation from Tyr-Pro dipeptide depends on whether the process takes place extra- or intracellularly.

The half-life of dipeptide in crude rat brain membrane preparation is 19.95 min (**79,82**); the rate of biodegradation in the cytoplasm is considerably faster (Tóth, Szemenyei, Rónai, unpublished) and unknown in the cerebrospinal fluid. This time factor should also be taken into consideration when calculating the time course of label incorporation into presumed precursor and the post-translational processing. Furthermore, if the incorporation of labeled tyrosine into large molecular weight precursor did take place, the appearance of labeled end-products should have increased by 60 min; in contrast, no significant radioactive peak was found in the extracts after 60 min even at very high detector amplification (in 4 out of 4 experiments). Taken together, weighing the data in the literature against the time course of incorporation of label into endomorphin-related end-products as found in the present series of experiments argues against the end-product generation via large molecular weight precursor.

Whereas, in the developed RIA measurement system to EM2 by us, R1 antiserum did not recognize natural or synthetic opioid peptide sequences unrelated to endomorhins. As judged from the recognition profile, it had good differentiation power for the C-terminal endomorphin motifs. Relevantly to the second EM2 immunoreactive peak, it did not react with synthetic EM2-OH. Therefore, the detected species must be a distinct, though, considering the similar retention pattern, structurally not an entirely unrelated one. We have

mentioned previously that in rats treated *icv* with [^{3}H]Tyr-Pro-OH, there was an incorporation of label into a peptide species with the retention time of authentic endomorphin 2 in RP-HPLC gradient separates and also at the retention time corresponding to EM2-OH. It is possible – though it is by no means proven – that the incorporation has happened into the novel immunoreactive species and not into authentic EM2-OH. Using commercial polyclonal antibody raised against EM2, Terskiy et al. (**163**) have reported four major immunoreactive protein bands in mouse brain lysates and three in human cell lines. The molecular size of these immunoreactive proteins (25–117 kDa range) renders it unlikely that any of these immunoreactive species would be even remotely related to the ones appearing in our RP-HPLC gradient separates.

The other possibility is de novo synthetic route, utilizing Tyr-Pro dipeptide precursor. According to the principles of enzymology, hydrolases – among them, peptidehydrolases – can theoretically operate both ways (i.e. as synthases as well) (**157-160**).

In the context of apparent presence of free carboxylic acid form of endomorphin 2 in brain extracts, one should recall that the major biotransformation route of endomorphins is a DPP-IV mediated cleavage between Tyr-Pro and Trp/Phe (**79,82**). Although carboxypeptidaseY and proteinase A can desaminate endomorphins into peptide acids, this is not a favoured biodegradation pathway, neither is any other carboxypeptidase action (**79,82**). Thus, the free carboxylic form (YPFF-OH) might be even a synthetic product on its own right. *If* there is an endogenous biosynthetic pathway for endomorphins utilizing Tyr-Pro substrate, it is likely to take place in a compartment where a peptidyl-glycine intermediate (**141,161,162**) formation can happen, with an amidated tetrapeptide as end-product.

4.4. Synthesis and ^{99m}Tc-labeling of annexin V fragments

Synthesis

Anx13, a peptide containing 13 amino acids was synthetized, corresponding to the sequency of the N-terminal of the Annexin V protein (Anx13: H-Ala-Gln-Val-Leu-Arg-Gly-Thr-Val-Thr-Asp-Phe-Pro-Gly-OH). The novel ^{99m}Tc-labeling methods require additional functional groups, hence derivatization of Anx13 on the N-terminal were carried out by attaching one or two cysteine (Cys-Anx13, Cys-Cys-Anx13), histidine (His-Anx13) or hydrasinonicotinic acid (HYNIC-Anx13).

Synthesis of annexin V fragment and its derivatives were performed by using solid phase peptide synthesis method on Merrifield resin, with Boc-chemistry. HYNIC-Anx13 was synthetized on 2-Chlorotrityl chloride resin using Fmoc strategy. The crude peptides were purified by RP-HPLC, using Vydac 218TP1010 semipreparative column. The identification

of the pure peptides were done by analytical RP-HPLC (Vydac 218TP54 column), using gradient elution (15%- 40% ACN /25 min,*10%-40%/40 min **10%- 35% ACN /30 min, flow rate: 1 cm^3/min). At the same time mass spectrum analysis was done as well (MALDI-TOF). R_f values were establish on silica gel 60 F_{254}-precoated glass plates. The solvent systems were following: (A) acetonitrile:methanol:water (4:1:1), (B) 1-butanol:acetic acid:water (2:1:1), (C) ethyl acetate:pyridine:acetic acid:water (60:20:6:11) (**Table 14**).

Peptides	TLC		HPLC	MS	
	R_f (A)	R_f (B)	k'	$[M+H]^+$	Mr
Anx13	0.27	0.63	3.91	1360.75	1359
Cys-Anx13	0.38	0.43	4.98	1463.81	1462
Cys-Cys-Anx13	0.27	0.38	7.46*	1566.92	1565
His-Anx13	0.40	0.23	4.35	1497.85	1496
HYNIC-Anx13	0.42	0.60	5.05**	1495.98	1494

Table 14. Analytical data of annexin V fragments, TLC: silica gel 60 F_{254}, solvent systems:
(A) pyridine/isoamyl alcohol/water (1:1:2),
(B) n-butanol/pyridine/acetic acid/water (15:3:8:10)

Stability studies

Long term stability studies proved that Anx13 is stable at least for one year when stored in refrigerator. Chromatograms indicating stability of Anx13 as a function of time can be seen in **Fig. 5.** Chromatographic conditions was the following: Vydac 218TP54 C18 reverse-phase column at a flow rate of 1 cm^3/min at ambient temperature. The mobile phase was mixed from 0.1% (v/v) TFA in water and 0.08% (v/v) TFA in ACN, and gradient elution was carried out from 15% to 40% of ACN within 25 min, UV detection was at 215 nm.

Stability results of derivatized Anx13 compounds are collected in **Table 15**. It can be seen that while histidine and cysteine derivatization does not affect on the stability of the peptides after 3 months, the cysteine-cysteine and HYNIC derivatization resulted in lower stability. The reason of the decreasing chemical purity of the cysteine-cysteine derivative can be explained by the opportunity of disulfide-bridge forming between the two –SH groups. On the other hand, this partial oxidation of –SH-groups led to an equilibrium: during the first month the amount of this impurity grew up to almost 20 %, while no significant increase of impurities was observed furtherly.

Since some novel technetium labeling method, e.g. nitrido labeling requieres elevated temperature, short time heat tolerance studies were performed with the cysteine derivatives of Anx13. In case of Cys-Cys-Anx13 solution, cca. 90 % of the peptide remained unchanged during 60 minutes when it was immersed into boiling water. MS data showed that this 10 %

decomposition corresponds to the loss of one cysteine, forming Cys-Anx13 compound. At the same time, no change was observed in case of Cys-Anx13 during the heat tolerance study.

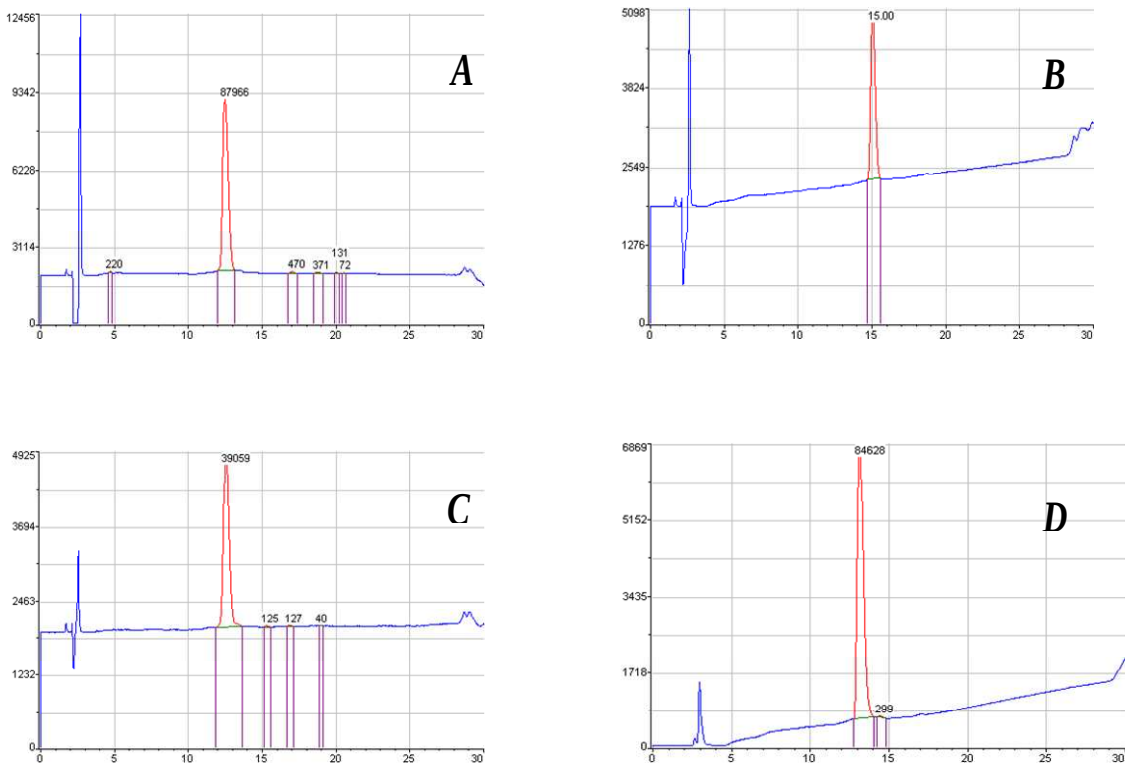

Figure. 5. Chromatograms of Anx13 **A**: at preparation, **B**: after 3 months, **C**: after 6 months, **D**: after 12 months. Purity was found higher than 96 % at any time

Compound	Purity after 3 months, %
Cys-Anx13	94.08
Cys-Cys-Anx13	80.80
His-Anx13	98.13
HYNIC-Anx13	85.13

Table 15. Stability of derivatized Annexin V fragments

Results and discussion of ^{99m}Tc-nitrido labeling

Both asymmetric and symmetric nitrido-labeling of Cys-Cys-Anx13 and asymmetric labeling of Cys-Anx13 have been carried out via ^{99m}Tc-nitrido ([^{99m}Tc≡N]) intermediate. For [^{99m}Tc≡N] intermediate 0.9 cm^3 (50 MBq) of $^{99m}TcO_4^-$ in saline was added to 1.1 cm^3 of SDH and $SnCl_2$ solution mixed from 1 cm^3 1mg/cm^3 SDH and 0.1 cm^3 1mg/cm^3 $SnCl_2$ and it was stirred at room temperature for 15 min.

On analysis by paper chromatography using acetone as mobile phase and Whatman ET-31 paper as support system, the free pertechnatate migrated with the solvent front (Rf ~1) the [^{99m}Tc≡N] intermediate remained at the point of spotting (Rf ~0) and ^{99m}Tc-nitrido intermediate could be prepared with >95% yields.

For symmetric labeling of Cys-Cys-Anx13, 0.25 mg of Cys-Cys-Anx13 in 0.5 cm^3 of saline was added to separate aliquots of 2 cm^3 of ^{99m}Tc-nitrido intermediate. The reaction mixtures were heated in boiling water bath for 1 h.

The Cys-Cys-Anx13 complexed with the ^{99m}Tc-nitrido intermediate in high yields (>95%) to form a single species as revealed by HPLC analysis (Rt: 11.5 min, result of A. Mukherjee). The probable structure of ^{99m}Tc-nitrido complex with Cys-Cys-Anx13 is given in **Fig. 6.** No radiochemical decomposition occured during two hours after the labeling.

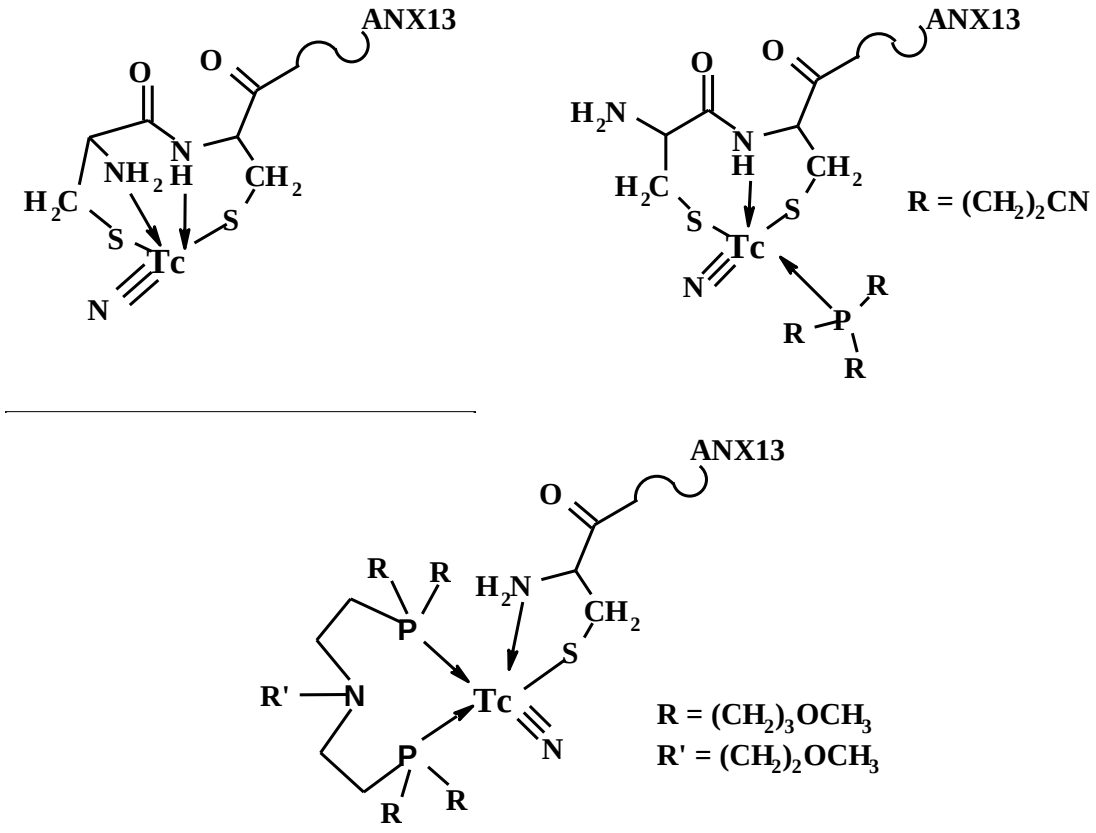

Figure 6. Probable sturcture of ^{99m}Tc-Cys-Cys-Anx13 (**A**), ^{99m}Tc-PCN-Cys-Cys-Anx13 (**B**), ^{99m}Tc-PNP-Cys-Anx13 (**C**)

For asymmetric labeling of Cys-Cys-Anx13, 0.25 mg of Cys-Cys-Anx13 in 0.5 cm^3 of saline, 0.5 mg of PCN in hydroxypropyl-γ-cyclodextrin (4 mg/cm^3 conc. saline solution) was reacted with the previously prepared ^{99m}Tc-nitrido intermediate at 100 ^{o}C for 1 hour.

Based on the TLC chromatograms it can be established that ^{99m}Tc-nitrido intermedier (**A,** Kieselgel 60/EtOH-water 1:1) is completely reacted with Cys-Cys-Anx13 and PCN by forming a single complex (**B,** Kieselgel 60/EtOH-water 1:1) and no free pertechnetate is present (**C,** ^{99m}Tc-PCN-Cys-Cys-Anx13 in Whatman ET-31 paper / acetone) (**Fig.7.**).

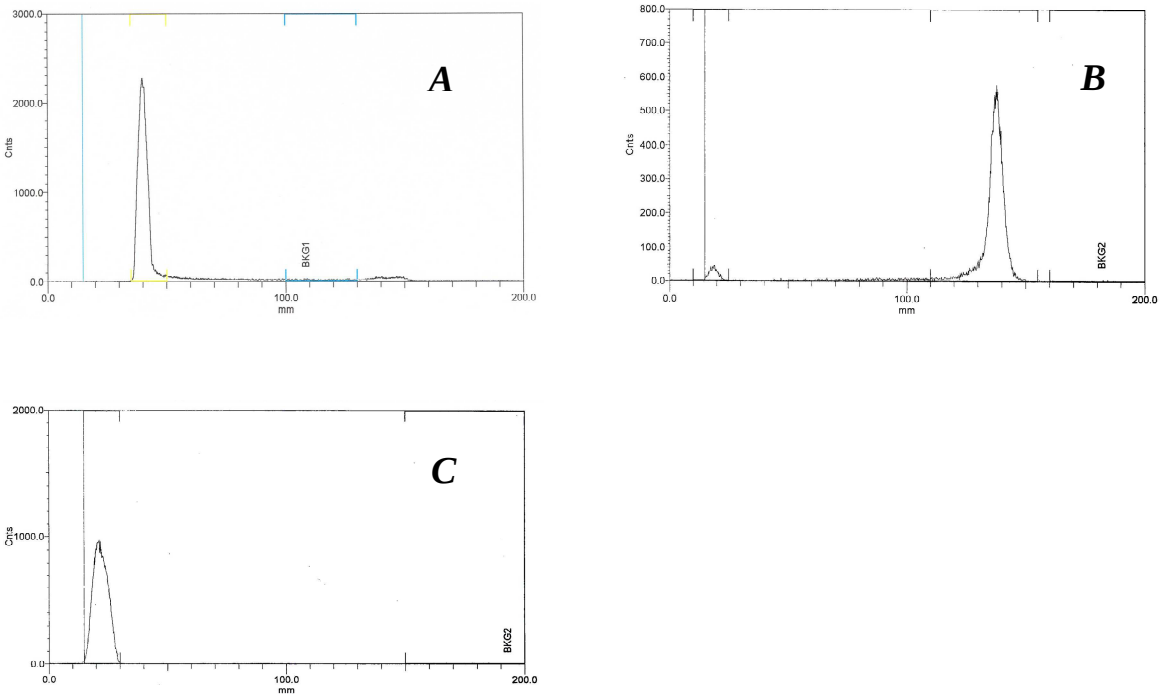

Figure 7. TLC chromatograms

For asymmetric labeling of Cys-Anx13, 0.01 cm^3 of PNP (~10 mg) was dissolved in 1 cm^3 ethanol in nitrogen atmosphere. 0.1 cm^3 of PNP was added to 1 cm^3 of ^{99m}Tc-nitrido intermediate along with 0.1 mg of C-Anx13 in 0.1 cm^3 of saline, and the reaction mixture was heated at 100 °C for 1 h (in Kanchan Kothari's laboratory).

The Cys-Anx13 reacted with ^{99m}Tc-nitrido intermediate in >95% yields. However, HPLC analysis of ^{99m}Tc-Cys-Anx13 revealed the formation of two species with retention times of 13.0 ± 0.2 and 14.3 ± 0.2 min. When attempts were made to prepare asymmetric complex via ^{99m}Tc-$(PNP)^{2+}$ fragment using diphosphine ligand, the complex ^{99m}Tc-PNP-Cys-Anx13 could be formed in >95% yields. But in this case also, HPLC analysis of the complex revealed the formation of two species with retention times of 18.0 ± 0.2 and 24 ± 0.2 min (results of A. Mukherjee).

Of three different ^{99m}Tc-nitrido-Anx13 complexes were studied, although all were formed in high yields of >95%, it was observed that ^{99m}Tc-Cys-Cys-Anx13 was formed as

single species, while ^{99m}Tc-PCN-Cys-Cys-Anx13 and ^{99m}Tc-PNP-Cys-Anx13 were formed with more than one species. Since complexes with multiple species are generally not acceptable as radiopharmaceuticals, owing to the possibility of differences in their pharmacokinetics (**164, 165**), these complexes were not evaluated for their biological behavior. Hence, in vitro studies were carried out only with ^{99m}Tc-Cys-Cys-Anx13 and ^{99m}Tc-$(CO)_3$-His-Anx13 (another ^{99m}Tc-Anx13 complex, synthesized via tricarbonyl precursor in Kanchan Kothari's laboratory) in apoptotic HL60 cells. Both ^{99m}Tc-Cys-Cys-Anx13 and ^{99m}Tc-$(CO)_3$-His-Anx13, which were proven to be single species, were found to be stable at room temperature for 24 h. ^{99m}Tc-Cys-Cys-Anx13 and ^{99m}Tc-$(CO)_3$-His-Anx13 were also stable and did not dissociate or transchelate when challenged with cysteine (0.1 M) and histidine (0.1 M) in saline, indicating their potential for further evaluation as apoptosis marker.

Among these, ^{99m}Tc-Cys-Cys-Anx13 exhibited specific uptake in apoptotic HL60 cells, which could be inferred from poor uptake in untreated HL60 cells as well as in treated cells in the presence of excess cold peptide Anx13. In the case of ^{99m}Tc-$(CO)_3$-His-Anx13, the uptake was higher but not found to be specific.

Among the four tested complexes, ^{99m}Tc-Cys-Cys-Anx13, which showed the best characteristics, was further evaluated in vivo in tumor-bearing Swiss mice to study its suitability to assess response to cancer therapy. ^{99m}Tc-Cys-Cys-Anx13 has shown reasonably good tumor uptake. Apart from the above, large molecules do not clear from the body quickly, often accompanied by soft tissue uptake of the radiopharmaceuticals.

In the case of ^{99m}Tc-HYNIC-annexin V too, earlier studies in normal Balb/c mice have shown high soft tissue retention and ^{99m}Tc-HYNIC-annexin V has also shown high retention of activity in the abdominal region in murine tumor model, making the product not suitable for evaluation of apoptosis in abdominal regions (**166**). In our studies with ^{99m}Tc-Cys-Cys-Anx13 in tumor-bearing Swiss mice, the retention in soft tissues is relatively low in comparison to ^{99m}Tc-HYNIC-annexin V (**167**). Thus, ^{99m}Tc-Cys-Cys-Anx13 could be a potential agent for apoptosis imaging.

5. Summary

Our aims were multiple, preparing of suitable tritium and ^{125}I-labeled peptides for *in vitro* or *in vivo* biological assays, development and application of a tritium labeled radioactive tracer for examination of a hypothesis, synthesis and derivatization of a putative biologically active protein fragments for novel ^{99m}Tc-labeling approaches.

Two Dmt^{1}-EM2 isotopomers were labeled with tritium in position 1 or position 2. Both radioligands exhibited high specific radioactivity. Different rates of degradation of EM2 and of Dmt^{1}-EM2 were observed in the rat brain homogenate. Dmt^{1}-EM2 was six times more resistant than EM2 to peptidases, the half-lives being 33.64 and 5.88 min, respectively. The half-life of [$^{3}H_2$]Pro^{2}-Dmt^{1}-EM2 proved almost 2.5 times longer than that of EM2. (**I.**)

To characterize the pharmacological properties of MEGY, a peptide in zebrafish, the organism in which this peptide is naturally present as an endogenous opioid ligand, we have labeled it with tritium ([^{3}H]MEGY). In addition, we have also synthesized two analogs: (D-Ala^{2})-MEGY (YaGFMGY) and (D-Ala^{2}, Val^{5})-MEGY (YaGFVGY). The binding profile of these three agents has been studied in zebrafish and rat brain membranes. [^{3}H]MEGY presents one binding site in zebrafish, as well as in rat brain membranes, although it shows a slight higher affinity in zebrafish brain. Competition binding assays indicate that the methionine residue is essential for high-affinity binding of MEGY and probably of other peptidic agonists in zebrafish, whereas the change of a Gly for a D-Ala does not dramatically affect the ligand affinity. (**II.**)

Since no genomic code has hitherto been found encoding for endomorphin precursor-like proteins. We have sought the possible indication of an alternative, *de novo* biosynthetic pathway, which is also an infrequent event in eukariotes (e.g. glutathione). Based on the hypothesis that biosynthesis of an oligopeptide may take place also from its fragments through a specific enzymatic route, we decided to test the probable incorporation of the tritiated Tyr-Pro dipeptide into endomorphin-related peptides. We found that radioactive peaks, matching the retention times of endomorphin-related tri- and tetrapeptides, are present in rat brain extracts following *icv* injection of [^{3}H]Tyr-Pro dipeptide. These labeled peptides appeared at 30 min but not 15 or 60 min after *icv* treatment, whereas labeled Tyr and/or Tyr-Pro could be detected both at 15 and 30 min. Radioactive peaks appeared with retention times matching that of co-injected free carboxylic form of endomorphin 2 (YPFF-OH, EM2-OH) in two extracts and a robust labeled peak in the position of endomorphin 2 standard in one sample. Although labeled peaks were regularly present in the tripeptide region, their exact matching with YPF or YPW could not be established. It might be of importance that no active peaks corresponding to endomorphin 1-related tetrapeptide standards were found. (**III.**)

By right of the total activity and specific activity of ^{125}I labeled endomorfin-2, the tracer proved to be suitable tool for radioimmunoassy measuring. Thus we developed a RIA protocol to endomorphin 2, and, in the course of selectivity profiling and validation of antisera in rat brain extracts, we found an EM2-immunoractive peak in the fraction corresponding to the retention time of standard EM2-OH in the RP-HPLC gradient separation system. Since the antiserum did not recognize authentic/standard EM2-OH, the immunoreaktive peak must be attributed to the presence of an as yet unidentified new EM2-like peptide.(**IV.**)

On the other hand, as it above mentioned, we found the incorporation of label into the purportedly same peaks, following *icv* injection of tritiated Tyr-Pro dipeptide into the lateral cerebral ventricle of rats. In both cases, identical extraction–purificationand RP-HPLC gradient separation conditions were used.

The N terminal chain of annexin V consisting of 13 amino acids, which is considered to bind to phosphatidylserine exposed on apoptotic cells, could be labeled with ^{99m}Tc using novel chemical approaches in ^{99m}Tc radiopharmaceutical chemistry. This study is the first one to report on the use of ^{99m}Tc-labeled annexin 13 fragment for apoptosis detection. Among the four different complexes tested, ^{99m}Tc-Cys-Cys-Anx13 has shown specific uptake in apoptotic human leukemia HL-60 cells in the in vitro studies. Biodistribution studies of ^{99m}Tc-Cys-Cys-Anx13 in tumorbearing Swiss mice also yielded encouraging results in tumor uptake and revealed superiority in soft tissue clearance in comparison with ^{99m}Tc-HYNIC annexin V. Being a small peptide that can be synthesized in large quantities, ^{99m}Tc-Cys-Cys-Anx13 warrants further evaluation for imaging apoptosis.(**V.**)

6. Reference list

1. G. Choppin, J.-O. Liljenzin, J. Rydberg; Radiochemistry and Nuclear Chemistry, Butterworth-Heinemann, Woburn, (Third Edition), (2002).

2. L.W. Alvarez, R. Cornog; *Phys. Rev.*, **56:** 613 (1939).

3. L. E. Feinendegen; Tritium-Labeled Molecules in Biology and Medicine, Academic Press, New York and London, (1967).

4. C. V. Cannon, E. M. Shapiro, G. H. Jenks, J. Boyle, L. T. McClinton, N. Elliott, C. J. Borkowski, H. S. Pomerance, R. P. Metcalf; The Production and Purification of Tritium, Clinton Laboratories, Oak Ridge, Tenn., (1957).

5. P. W. Frank; Determination of the Effective Neutron Flux for Prodution of Tritium from LiOH in Primary Coolant of PWR, Westinghouse Electric Corp., Bettis Atomic Power Div., Pittsburgh, (1958).

6. N. Chellew, J. McGuire, W. Olsen, A. H. Barnes; Tritium Production Process, Argonne National Laboratory, Illinois, (1960).

7. W. M. Jones; *Phys. Rev.*, **100:** 124 (1955).

8. E. A. Evans; *Atomic Energy*, **24**: 262 (1968).

9. E. A. Evans, D. C. Warrell, J. A. Elvidge, J. R. Jones; *Handbook of Tritium NMR Spectroscopy and Applications*, John Wiley and Sons Inc, New York, (1985).

10. G. Tóth, S. Lovas, F. Ötvös; In *Meth. in Mol. Biol., Neuropept. Prot.*, **73**: 219 (1997).

11. K. E. Wilzbach; *J. Am. Chem. Soc.*, **79**: 1013 (1957).

12. J. Oehlke, E. Mittag, G. Tóth, M. Bienert, H. Niedrich; *J. Labelled Compd. Radiopharm.*, **24**: 1483 (1987).

13. K. Nägren, H. M. Franzén, U. Ragnarsson, B. Längström; *J. Labelled Compd. Radiopharm.*, **25**: 141 (1988).

14. D. Cooper, E. Reich; *J. Biol. Chem.*, **247**: 3008 (1972).

15. P. J. Franker, J. C. Speck; *Biochem. Biophys. Res. Commun.*, **80**: 849 (1978).

16. B. Búzás, G. Tóth, S. Cavagnero, V. J. Hruby, A. Borsodi; *Life Sci.*, **50**: 75 (1992).

17. A. Y. L. Shu, R. Heys; In *Synth. and Appl. of Isotopically Labelled Compd.*, Elsevier, Amsterdam, pp 85 (1991).

18. R. S. P. Hsi, W. T. Stolle, G. L. Bundy; *J. Labelled Compd. Radiopharm.*, **24**: 1175 (1994).

19. C. Perrier, E. Segré; *Nature*, **140**: 193 (1937).

20. C. Perrier, E. Segré; *J. Chem. Phys.*, **5**: 712 (1937).

21. E. Segré, C. S. Wu; *Phys. Rev.*, **57**: 552 (1940).

22. F. A. Paneth; *Nature*, **159**: 8 (1947).

23. G. T. Seaborg, E. Segré; *Phys. Rev.*, **55**: 808 (1939).

24. *Nature's Building Blocks*, page 423, paragraph 2

25. V. J. Molinski; *Int. J. Appl. Radiat. Isot.*, **33**: 811 (1982).

26. E. A. Deutsch, K. Libson, S. Jurisson; *Progress in Inorganic Chemistry*, John Wiley and Sons Inc, New York, pp 75 (1983).

27. S. Liu, D. S. Edwards; *Chem. Rev.*, **99**: 2235 (1999).

28. M. J. Abrams, M. Juwied, C. I. TenKate, D. Schwartz, M. M. Hauser, F. E. Gaul, A. J. Fuccello, R. H. Rubin, H. W. Strau, A. J. Fischman; *J. Nucl. Med.*, **31**: 2022 (1990).

29. J. W Babich., H. Solomon, M. C. Pike, D. Kroon, W. Graham, M. J. Abrams, R. G. Tompkins, R. H. Rubin, A. J. Fischman; *J. Nucl. Med.*, **34**: 964 (1993).

30. S. Banerjee, M. R. A. Pillai, N. Ramamoorthy; *Semin. in Nucl. Med.*, **31**: 260 (2001).

31. A. Duatti, A. Boschi, L. Uccelli; *Braz. Arch. Biol. Tech.*, **45**: 135 (2002).

32. A. Duatti, C. Bolzati, L. Uccelli, G. L. Zucchini; *Transition Met. Chem.*, **22**: 313 (1997).

33. F. Daghighian, E. Barendswaard, S. Welt, J. Humm, A. Scott, M. C. Willingham, E. McGuffie, L. J. old, S. M. Larson; *J. Nucl. Med.*, **37**: 1052 (1996).

34. A. I. Kassis, K. S. R. Sastry, S. J. Adelstein; *Radiat. Res.*, **109**: 78 (1987).

35. P. V. Harper, W. D. Siemens, K. A. Lathrop, H. E. Brizel, R. W. Harrison; Iodine-125. Proc. Japan Conf. Radioisotopes, (1961).

36. D. R. Lide, N. E. Holden; In *CRC Handbook of Chemistry and Physics, 85th Edition*. CRC Press. Boca Raton, Florida, (2005).

37. W. M. Hunter, F. C. Greenwood; *Nature* **194**: 495 (1962).

38. P. R. P. Salacinski, C. McLean, J. E. C. Sykes, V. V. Clement-Jones, P. J. Lowry; *Anal. Biochem.*, **117**: 136 (1981).

39. J. J. Marchalonis; *Biochem. J.*, **113**: 299 (1969).

40. M. A. K. Markwell; *Anal. Biochem.*, **125**: 427 (1982).

41. J. B. Tatro, S. Reichlin; *Endocrinology*, **121**: 1900 (1987).

42. A. E. Bolton, W. M. Hunter; *Biochem J.*, **133**: 529 (1973).

43. M. Gates, G. Tschudi; *J. Am. Chem. Soc.*, **78**: 1380 (1956).

44. H. McQuay; *Lancet*, 353: 2229 (1999).

45. A. H. Beckett, A. F. Casy; *J. Pharm. Pharmacol.*, **6**: 986 (1954).

46. A. D. Corbett, G . Henderson, A. T. McKnight, S. J. Paterson; *Brit. J. Pharmacol.*, **147**: S153 (2006).

47. C. J. Evans, D. E. Keith, H. Morrison, K. Magendzo, R. H. Edwards; *Science*, **258**: 1952 (1992).

48. B. L. Kieffer, K. Befort, C. Gaveriaux-Ruff, C. G. Hirth; *Proc. Natl. Acad. Sci. USA,* **89**: 12048 (1992).

49. Y. Chen, A. Mestek, J. Liu, J. A. Hurley, L. Yu; *Mol. Pharmacol.*, **44**: 8 (1993).

50. M. Minami, T. Toya, Y. Katao, K. Maekawa, S. Nakamura, T. Onogi, S. Kaneko, M. Satoh; *FEBS Lett.*, **329**: 291 (1993).

51. C. Mollereau, M. Parmentier, P. Mailleux, JL. Butour, C. Moisand, P. Chalon, D. Caput, G. Vassart, JC. Meunier; *FEBS Lett.*, **341**: 33 (1994).

52. S. Nakanishi, A. Inoue, T. Kita, A. Inoue, M. Nakamura, A. C. Y. Chang, S. N. Cohen, S. Numa; *Nature*, **278**: 423 (1979).

53. H. Kakidani, Y. Furutani, H. Takahashi, M. Noda, Y. Morimoto, T. Hirose, M. Asai, S. Inayama, S. Nakanishi, S. Numa; *Nature*, **298**: 245 (1982).

54. M. Noda, Y. Furutani, H. Takahashi, M. Toyosato, T. Hirose, S. Inayama, S. Nakanishi, S. Numa; *Nature*, **295**: 202 (1982).

55. J. C. Meunier, C. Mollereau, L. Toll, C. Suaudeau, C. Moisand, P. Alvinerie, J. L. Butour, J. C. Guillemot, P. Ferrara, B. Monsarrat, H. Mazarguil, G. Vassart, M. Parmentier, J. Costentin; *Nature*, **377**: 532 (1995)

56. H. W. Kosterlitz , S. J. Paterson; *Philos. Trans. R. Soc. Lond. B. Biol. Sci.*, **308**: 291 (1985).

57. A. D. Corbett, S. J. Paterson, H. W. Kosterlitz; *In: Handbook of Exp. Pharmacol.*, **104/1**: 645 (1993).

58. R. K. Reinscheid, H. P. Nothacker, A. Bourson, A. Ardati, R. A. Henningsen, J. R. Bunzow, D. K. Grandy, H. Langen, F. J. Monsma, Jr., O. Civelli; *Science*, **270**: 792 (1995)

59. J. E. Zadina, L. Hackler, L. J. Ge, A. J. Kastin; *Nature*, **386**: 499 (1997)

60. H. Teschemacher, G. Koch, V. Brantl; *Biopolymers*, **43**: 99 (1997).

61. V. Brantl, C. Gramsch, F. Lottspeich, R.Mertz, K.-H. Jaeger, A. Herz; *Eur. J. Pharmacol.*, **125**: 309 (1986).

62. E. Kostyra, E. Sienkiewicz-Szłapka, B. Jarmołowska, S. Krawczuk, H. Kostyra; *Pol. J. Food Nutr. Sci.*, **13/54**: 25 (2004).

63. H. Meisel, R. J. FitzGerald; *Br. J. Nutr*., **84**: 27 (2000).

64. F. Nyberg, K. Sanderson, E.L. Glämsta; *Biopolymers*, **43:** 147 (1997).

65. S. Moisan, N. Harvey, G. Beaudry, P. Forzani, K.E. Burhop, G. Drapeau, F. Rioux; *Peptides*, **19**: 119 (1998).

66. E. Blishchenko, O. Sazonova, A. Surovoy, S. Khaidukov,Y. Sheikine, D. Sokolov, I. Freidlin, M. Philippova, A. Vass, A. Karelin, V. Ivanov; *J. Pept. Sci*., **8**: 438. (2002).

67. V. Erspamer, P. Melchiorri; *Trends Pharmacol. Sci.,* **1**: 391 (1980).

68. V. Erspamer , P. Melchiorri, G. Falconieri-Erspamer, L. Negri, R. Corsi, C. Severini, D. Barra, M. Simmaco, G. Kreil; *Proc. Natl. Acad. Sci. USA,* **86**: 5188 (1989).

69. M. Amiche, A. Delfour, P. Nicolas; *EXS,* **85**: 57 (1998).

70. M. Broccardo, V. Erspamer, G. Falconieri Erspamer,G. Improta, G. Linari, P. Melchiorri, P. C. Montecucchi; *Br. J. Pharmacol.,* **73**: 625 (1981).

71. P. Pattee, A.-E. Ilie, S. Benyhe, G. Toth, A. Borsodi, S. R. Nagalla; *J. Biol. Chem.,* **278**: 53098 (2003).

72. C. W. Stevens, G. Toth, A. Borsodi, S. Benyhe; *Brain Res. Bull.,* **71**: 628 (2007).

73. L. Hackler, J. E. Zadina, L.-J. Ge, A. J. Kastin; *Peptides*, **18**: 1635 (1997).

74. M. Schreff, S. Schulz, D. Wiborny, V. Höllt; *Neuroreport,* **9**: 1031 (1998).

75. S. Martin-Schild, A. A. Gerall, A. J. Kastin, J. E. Zadina; *J. Comp. Neurol.,* **405**: 450 (1999).

76. T. L. Pierce, M. W. Wessendorf; *J. Chem. Neuroanat.,* **18**: 181 (2000).

77. R. Shane, S. Wilk, R. J. Bodnar; *Brain Res.,* **815:** 278 (1999).

78. C. Sakurada, S. Sakurada, T. Hayashi, S. Katsuyama, K. Tan-No, T. Sakurada; *Biochem. Pharmacol.,* **66:** 653 (2003).

79. C. Tomboly, A. Peter, G. Toth; *Peptides,* **23:**1573 (2002).

80. A. Janecka, R. Kruszynski, J. Fichna, P. Kosson, T. Janecki; *Peptides*, **27:** 131 (2006).

81. P. F. Berne, J. M. Schmitter, S. Blanquet; *J. Biol. Chem.,* **265:** 19551 (1990).

82. A. Peter, G. Toth, C. Tomboly, G. Laus, D. Tourwe; *J. Chrom. A.,* **846:** 39 (1999).

83. J. Gong, J. A. Strong, S. Zhang, X. Yue, R. N. DeHaven, J. D. Daubert, j. A. Cassel, G. Yu, E. Mansson, L. Yu; *FEBS Lett.,* **439**: 152 (1998).

84. A. Janecka, R. Staniszewska, J. Fichna; *Curr. Med. Chem.,* **14**: 1 (2007).

85. B. Leitgeb; *Chem. Biodiv.,* **4**: 2703 (2007).

86. J. D. W. Hansen, A. Stapelfeld, M. A. Savage, M. Reichman, D. L. Hammond, R. C. Haaseth, H. I. Mosberg; *J. Med. Chem.,* **35**: 684 (1992).

87. S. Salvadori, A. Martti, G. Balboni, C. Bianchi, S. D. Bryant, O. Crescenzi, R. Guerrini, D. Picone, T. Tancredi, P.A. Temussi, L. H. Lazarus; *Mol. Med.,* **1**: 678 (1995).

88. R. Guerrini, A. Capasso, L. Sorrentino, R. Anacardio, S. D. Bryant, L. H. Lazarus A. Martti, S. Salvadori; *Eur. J. Pharmacol.* **302:** 37 (1996).

89. S.D. Bryant, S. Salvadori, P. S. Cooper, L. H. Lazarus; *Trends Pharmacol. Sci.,***19**: 42 (1998).

90. Y. Sasaki, T. Suto, A. Ambo, H. Ouchi, Y. Yamamoto; *Chem. Pharm. Bull.,* **47**: 1506 (1999).

91. P. W. Schiller, T. M. Nguyen, I. Berezowska, S. Dupuis, G. Weltrowska, N. N. Chung, C. Lemieux; *Eur. J. Med. Chem.,* **35**: 895 (2000).

92. G. Balboni, S. Salvadori, R. Guerrini, L. Negri, E. Giannini, Y. Jinsmaa, S.D. Bryant, L.H. Lazarus; *J. Med. Chem.,* **45**: 5556 (2002).

93. D. Bryant, Y. Jinsmaa, S. Salvadori, Y. Okada, L. H. Lazarus; *Biopolymers (Pept. Sci.),* **71**: 86 (2003).

94. Y. Okada, Y. Tsuda, Y. Fujita, T. Yokoi, Y. Sasaki, A. Ambo, R. Konishi, M. Nagata, S. Salvadori, Y. Jinsmaa, S. D. Bryant, L. H. Lazarus; *J. Med. Chem.,* **46:** 3201 (2003a).

95. Y. Fujita, Y. Tsuda, T. Li, T. Motoyama, M. Takahashi, Y. Shimizu, T. Yokoi, Y. Sasaki, A. Ambo, A. Kita, Y. Jinsmaa, S. D. Bryant, L. H. Lazarus, Y. Okada; *J. Med. Chem.,* **47**: 3591 (2004).

96. Y. Okada, Y. Fujita, T. Motoyama, Y. Tsuda, T. Yokoi, T. Li, Y. Sasaki, A. Ambo, Y. Jinsmaa, S. D. Bryant, L. H. Lazarus; 2003b. *Bioorg. Med. Chem.,* **11:** 1983 (2003b).

97. K. Befort, L. Tabbara, D. Kling, B. Maigret, B. L. Kieffer; *J. Biol. Chem.,* **271**: 10161 (1996).

98. I. Alkorta, G. H. Lowe; *Protein Eng.,* **9**: 573 (1996).

99. G. Golling, A. Amsterdam, Z. Sun, M. Antonelli, E. Maldonado, W. Chen, S.Burgess, M. Haldi, K. Artzt, S. Farrington, S.-Y. Lin, R. M. Nissen, N. Hopkins; *Nat. Genet*., **31:**135 (2002).

100. T. Darland, J. E. Dowling; *Proc. Natl. Acad. Sci. USA,* **98:** 11691 (2001).

101. C. A. Dlugos, R. A. Rabin; *Pharmacol. Biochem. Behav.,* **74:** 471 (2003).

102. F. B. Pichler, S. Laurenson, L. C. Williams, A. Dodd, B. R. Copp,D. R. Love; *Nat. Biotechnol.,* **21:** 879 (2003).

103. V. Gonzalez-Nunez, R. Gonzalez-Sarmiento, R. E. Rodriguez; *Mol. Brain. Res.,* **114:** 31 (2003a).

104. V. Gonzalez-Nunez, R. Gonzalez-Sarmiento, R. E. Rodriguez; *BBA Gene Struct. Expr.*, **1629:** 114 (2003b).

105. V. Gonzalez-Nunez, R. Gonzalez-Sarmiento, R. E. Rodriguez; *Mol. Brain. Res.,* **120:** 1 (2003c).

106. M. Leist, M. Jaattela; *Nat. Rev. Mol. Cell. Biol.*, **2**: 589 (2001).

107. J. F. Kerr; *J. Path. Bact.,* **90**: 419 (1965).

108. J. F. Kerr, A. H. Wyllie, A. R. Currie; *Br. J. Cancer,* **26**: 239 (1972).

109. V. A. Fadok, D. R. Voelker, P. A. Campbell, J. J. Cohen, D. L. Bratton, P. M. Henson; *J. Immunol*., **148**: 2207 (1992).

110. M. O. Li, M. R. Sarkisian, W. Z. Mehal, P. Rakic, R. A. Flavell; *Science,* **302**: 1560 (2003).

111. X. Wang, Y.-C. Wu, V. A. Fadok, M.-C. Lee, K. Gengyo-Ando, L.-C. Cheng, D. Ledwich, P.-K. Hsu, J.-Y. Chen, B.-K. Chou, P. Henson, S. Mitani, D. Xue; *Science*, **302**: 1563 (2003).

112. J. Savill, C. Gregory, C. Haslett; *Science* **302**: 1516 (2003).

113. L. Hofstra, I. H. Liem, E. A. Dumont, H. H. Boersma, W. L. van Heerde, P. A. Doevendans, E. DeMuinck, H. J. J. Wellens, G. J. Kemerink, C. P. M. Reutelingsperger, G. A. Heidendal; *Lancet*, **356**: 209 (2000).

114. E. A. Dumont, C. P. Reutelingsperger, J. F. Smits, M. J. A. P. Daemen, P. A. F. Doevendans, H. J. J. Wellens, L. Hofstra; *Nat. Med*., **7**: 1352 (2001).

115. E. A. Dumont, L. Hofstra, W. L. van Heerde, S. van den Eijnde, P. A. F. Doevendans, E. DeMuinck, M. A. R. C. Daemen, J. F. M. Smits, P. Frederik, H. J. J. Wellens, M. J. A. P. Daemen, C. P. M. Reutelingsperger; *Circulation*, **102**: 1564 (2000).

116. F. G. Blankenberg, P. D. Katsikis, J. F. Tait, R. E. Davis, L. Naumovski, K. Ohtsuki, S. Kopiwoda, M. J. Abrams, M. Darkes, R. C. Robbins, H. T. Maecker, H. W. Strauss; *Proc. Natl. Acad. Sci. USA*, **95**: 6349 (1998).

117. G. Koopman, C. P. Reutelingsperger, G. A. Kuijten, R. M. Keehnen, S. T. Pals, M. H. van Oers; *Blood*, **84**: 1415 (1994).

118. V. Gerke, S. E. Moss; *Physiol. Rev*., **82**: 331 (2002).

119. S. E. Moss, R. O. Morgan; *Genome Biol.,* **5**: 219 (2004).

120. U. Grundmann, K.-J. Abel, H. Bohn, H. Lobermann, F. Lottspeich, H. Kupper; *Proc. Natl. Acad. Sci. USA*, **85**: 3708 (1988).

121. R. Huber, R. Berendes, A. Burger, M. Schneider, A. Karshikov, H. Luecke, J. Römisch, E. Paques; *J. Mol. Biol.,* **223**: 683 (1992).

122. C. Pigault, A. Follenius-Wund, M. Schmutz, J.-M. Freyssinet, A. Brisson; *J. Mol. Biol.*, **236**: 199 (1994).

123. P. Meers, T. Mealy; *Biochemistry*, **32**: 11711 (1993).

124. M. van Engeland, H. J. Kuijpers, F. C. Ramaekers, C. P. Reutelingsperger, B. Schutte; *Exp. Cell. Res*., **235**: 421 (1997).

125. H. Kenis, H. van Genderen, A. Bennaghmouch, H. A. Rinia, P. Frederik, J. Narula, L. Hofstra, C. P. M. Reutelingsperger; *J. Biol. Chem*., **279**: 52623 (2004).

126. P. W. Vriens, F. G. Blankenberg, J. H. Stoot, K. Ohtsuki, G. J. Berry, J. F. Tait, H. W. Strauss, R. C. Robbins; *J. Thorac. Cardiovasc. Surg*., **116**: 844 (1998).

127. A. M. Post, P. D. Katsikis, J. F. Tait, S. M. Geaghan, H. W. Strauss, F. G. Blankenberg; *J. Nucl. Med.*, **43**: 1359 (2002).

128. M. Subbarayan, U. O. Hafeli, D. K. Feyes, J. Unnithan, S. N. Emancipator, H. Mukhtar; *J. Nucl. Med.*, **44**: 650 (2003).

129. A. M.Green, N. D. Steinmetz; *Cancer J.*, **8**: 82 (2002).

130. A.M. Post, P. D. Katsikis, J. F. Tait, S. M. Geaghan, H. W. Strauss, F. G. Blankenberg; *J. Nucl. Med.*, **43**:1359 (2002).

131. F. G. Blankenberg, L. Naumovski, J.F. Tait , A. M. Post, H. W. Strauss; *J. Nucl. Med.*, **42**: 309 (2001).

132. S. Zijlstra, J. Gunawan, W. Burchert; *Appl. Radiat. Isot.*, **58**: 201 (2003).

133. J. Toretsky, A. Levenson, I. N. Weinberg, J. F. Tait, A. Uren, R. C. Mease; *Nucl. Med. Biol.*, **31**: 747 (2004).

134. P. McQuade, L. A. Jones, J. L.Vanderheyden, M. J. Welch; *J. Labelled Compd. Radiopharm.*, **46**: S1(2003).

135. B. Dekker, H. Keen, D. Shaw, L. Disley, D. Hastings, J. Hadfield; *Nucl. Med. Biol.*, **32**: 403 (2005).

136. M. Glaser, D. R. Collingridge, E.O. Aboagye, L. B. Hayes, O. C. Hutchinson, S. J. Martin, *Appl. Radiat. Isot.*, **58**: 55 (2003).

137. C. Lahorte, G. Slegers, J. Philippe, C. van de Wiele, R. A. Dierckx; *Biomol. Eng.*, **17**: 51 (2001).

138. J. Russell, J. A. O'Donoghue, R. Finn, J. Koziorowski, S. Ruan, J. L. Humm; *J. Nucl. Med.*, **43**: 671 (2002).

139. F. G. Blankenberg, P. D. Katsikis, J. F. Tait, R. E. Davis, L. Naumovski, K. Ohtsuki; *Proc. Natl. Acad. Sci. USA*, **95**: 6349 (1998).

140. L. Hoftstra, I. H. Liem, E. A. Dumont, H. H. Boersma, W. L. van Heerde, P. A. Doevendans; *Lancet*, **356**: 209 (2000).

141. Y. P. Loh, D. C. Parish; *In: Neuropeptides and their peptidases*. Chichester' Ellis Horwood Ltd.; 65–84 (1987).

142. B. F. Gisin; *Helv. Chim. Acta*., **56**: 1476 (1973).

143. E. Kaiser, R. L. Colescott, C. D. Bossinger, P. I. Cook; *Anal. Biochem.*, **34**: 595 (1970).

144. S. Baba, H. Hasegawa, Y. Shinohara; *J. Labelled Compd. Radiopharm.*, **27**: 1359 (1989).

145. S. Einarsson, S. Folestad, B. Josefsson, S. Lagerkvist; *Anal. Chem.*, **58**: 1638 (1986).

146. A.J. Czernik, B. Petrack; *J. Biol. Chem.*, **258**: 5525 (1983).

147. T. L. Goodfriend, L. Levine, G. D. Fasman; *Science,* **144**:1344(1964).

148. C. Tomboly, R. Dixit, I. Lengyel, A. Borsodi, G.Tóth, *J. Labelled Compd. Radiopharm.*, **44**: 355 (2001).

149. V. Gonzalez-Nunez, R. Gonzalez-Sarmiento, R. E. Rodriguez; *Mol. Brain. Res.*, **114**: 31 (2003).

150. V. Gonzalez-Nunez, A. Barrallo, J.R. Traynor, R. E. Rodriguez; *J. Pharmacol. Exp. Ther.*, **316**: 900 (2005).

151. K. J. Chang, E. Hazum, P. Cuatrecasas; *Proc. Natl. Acad. Sci. USA*, **78**: 4141(1981).

152. I. S. Zagon, M. F. Verderame, P.J. McLaughlin; *Brain. Res. Rev.*, **38**: 351 (2002).

153. R. E. Mains, B. A. Eipper; *J. Biol. Chem.*, **253**: 651 (1978).

154. R. E. Mains, B. A. Eipper; *In: Endorphins '78.* Budapest' Publishing House of Hungarian Academy of Sciences; p. 79–120 (1979).

155. J. F. Habener, J. T. Potts, A. Rich Jr.; *J. Biol. Chem.*, **251**: 3893 (1976).

156. D. F. Steiner, W. Kemmler, H. S. Tager, J. D. Peterson; *Fed. Proc.*, **33**: 2105 (1974).

157. U. Eichhorn, A. S. Bommarius, K. Drauz, H. D. Jakubke; *J. Pept. Sci.*, **3**: 245 (1997).

158. A. Murphy, C. O Fagain; *Essays Biochem.*, **31**:61 (1996).

159. M. Schuster, A. Aaviksaar, M. Haga, U. Ullmann, H. D. Jakubke; *Biomed. Biochim. Acta.*, **50**: S84 (1991).

160. H. Kleinkauf, H. von Dohren; *Eur. J. Biochem.*, **192**:1 (1990).

161. S. L. Milgram, S. T. Kho, G. V. Martin, R. E. Mains, B. A. Eipper; *J. Cell. Sci.*, **110**: 695 (1997).

162. R. Meskini, R. E. Mains, B. A. Eipper; *Endocrinology*, **141**: 3020 (2000).

163. A. Terskiy, K. M. Wannemacher, P. N. Yadav, M. Tsai, B. Tian, R. D. Howells; *Life Sci.*, **81**:1593 (2007).

164. R. Hom, J. Katzenellenbogen; *Nucl. Med. Biol.*, **24**: 485 (1997).

165. J. R. Dilworth, S. Parrot; *Chem. Soc. Rev.*, **27**: 43 (1998).

166. M. Subbarayan, U. O. Hafeli, D. K. Feyes, J. Unnithan, S. N. Emancipator, H. Mukhtar; *J. Nucl. Med.*, **44**: 650 (2003).

167. F. G. Blankenberg, P. D.Katsikis, J. F. Tait, R. E. Davis, L. Naumovski, K. Ohtsuki, S. Kopiwoda, M. J. Abrams, H. W. Strauss; *J. Nucl. Med.*, **40**:184 (1999).